125(+1) years of X-ray imaging…
…and still eager to push further

Marco Stampanoni

Institute for Biomedical Engineering, University and ETH Zürich, Zürich, Switzerland
Swiss Light Source, Paul Scherrer Institut, Villigen, Switzerland

X-ray radiography yesterday

X-ray micro-radiography of a fruit fly

Muscles and tracheal network *during* flight


NewScientist Life

Home News In-Depth Articles Opinion CultureLab Galleries Topic Guid

SPACE TECH ENVIRONMENT HEALTH LIFE PHYSICS&MAT

Home | Life | News

Surreal X-ray movie reveals how a fly beats its wings

21:00 25 March 2014 by Jacob Aron
For similar stories, visit the Picture of the day Topic Guide

BBC Sign in News Sport Weather Shop

NEWS

Home Video World UK Business Tech Science Magazine

Science & Environment

Scientists film inside a flying insect

By Victoria Gill
Science reporter, BBC News

26 March 2014 | Science & Environment

Walker et al., PloS Biology (2014) & Mokso et al., SciRep (2015)

X-ray sources of the 21st century

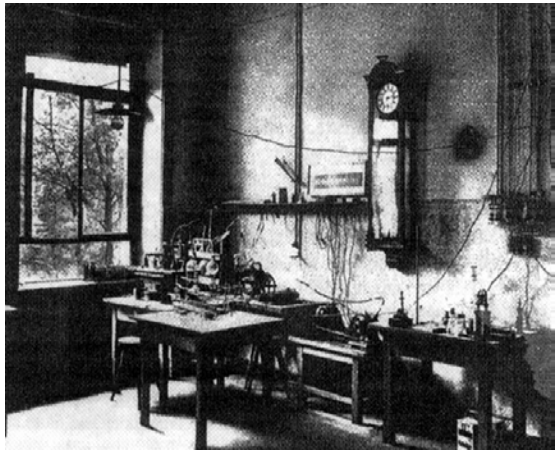

Röntgen's Lab, late 19th century

$$B \propto \frac{\text{Flux}}{\sigma_x \sigma_y \delta\theta_x \delta\theta_y}$$

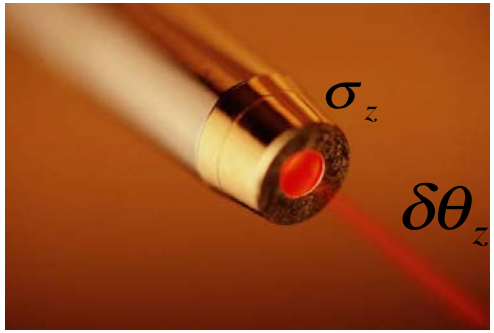

Swiss Light Source, today

Brilliance!

Brilliance over the last century: the enabler!

1000-500 µm

Hospital

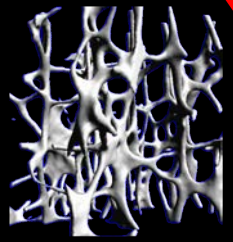

50-10 µm

Table Top micro CT

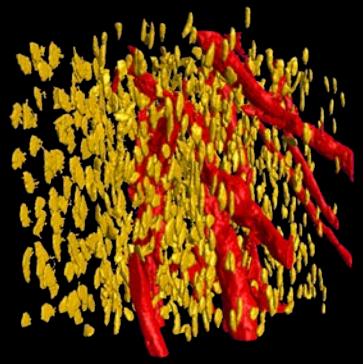

1-0.1 µm

SR - Tomographic Microscopy

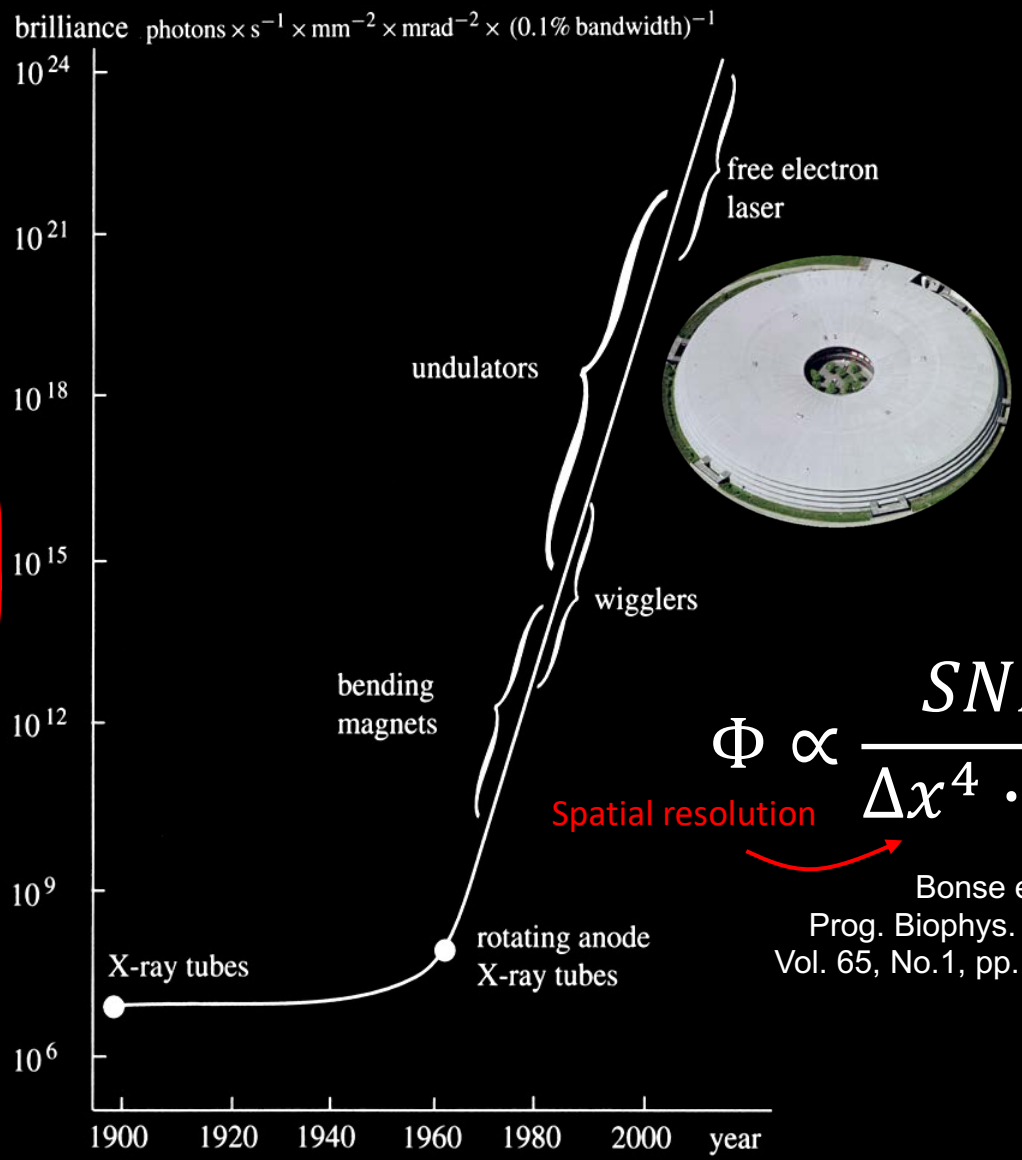

Contrast

$$\Phi \propto \frac{SNR^2}{\Delta x^4 \cdot \Delta \mu^2}$$

Spatial resolution

Bonse et al.,
Prog. Biophys. Molec. Biol.,
Vol. 65, No.1, pp. 133-169, 1996

The Swiss Light Source

Machine:

- 100 MeV Linac
- 2.4 GeV Booster
- 2.4 GeV Storage ring
- 400 mA e-current

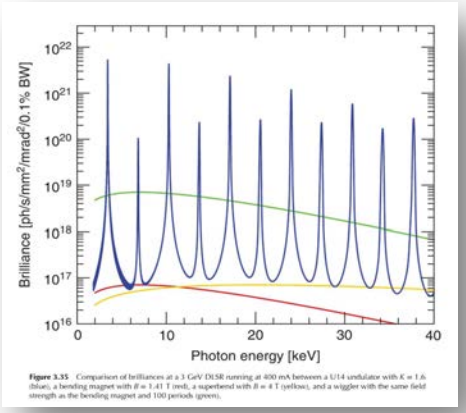

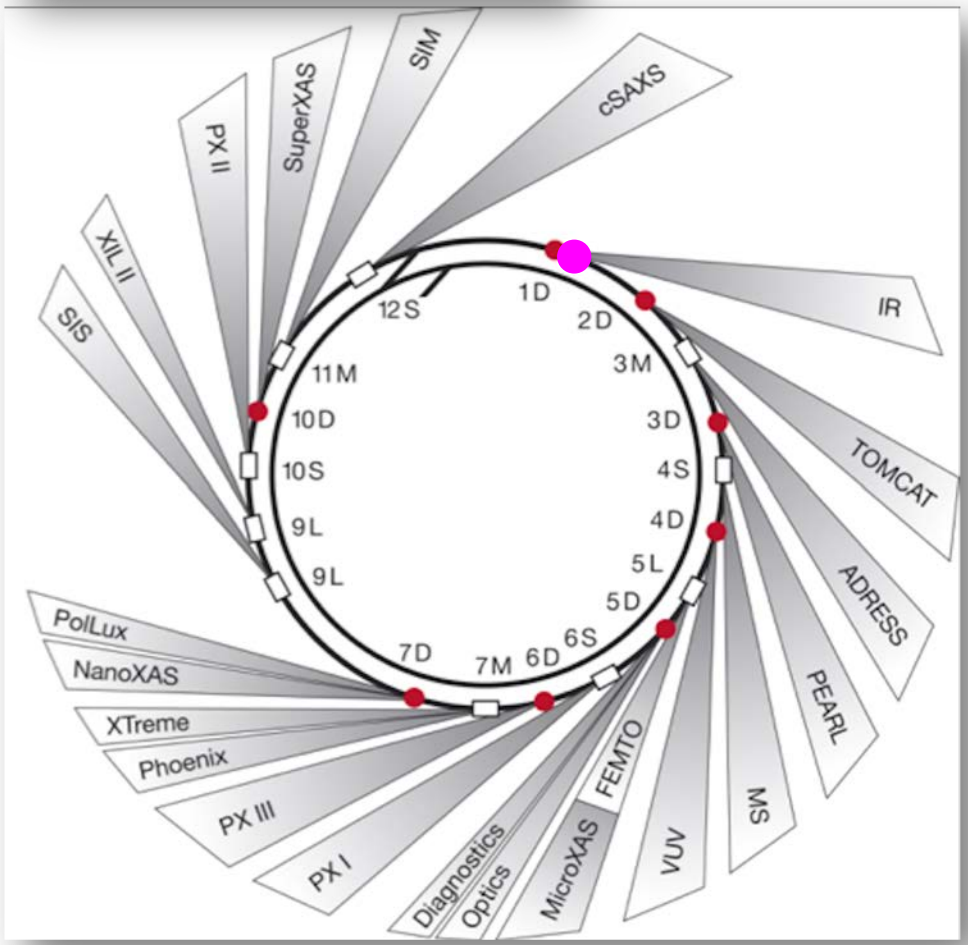

http://sls.web.psi.ch/view.php/beamlines/index.html

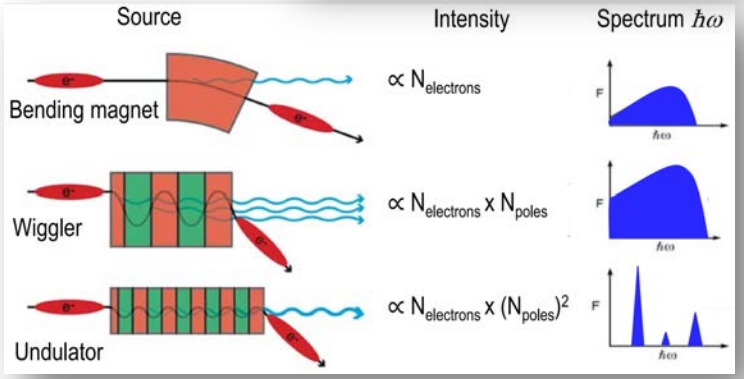

https://physics.stackexchange.com/

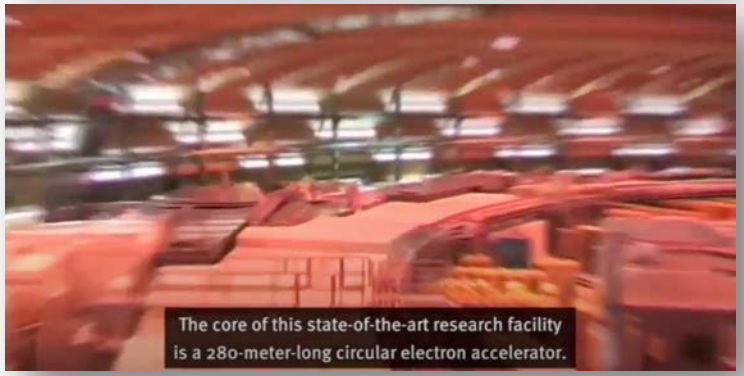

https://youtu.be/nXmLGV9zVkA

A beamline shapes the synchrotron radiation to users's needs

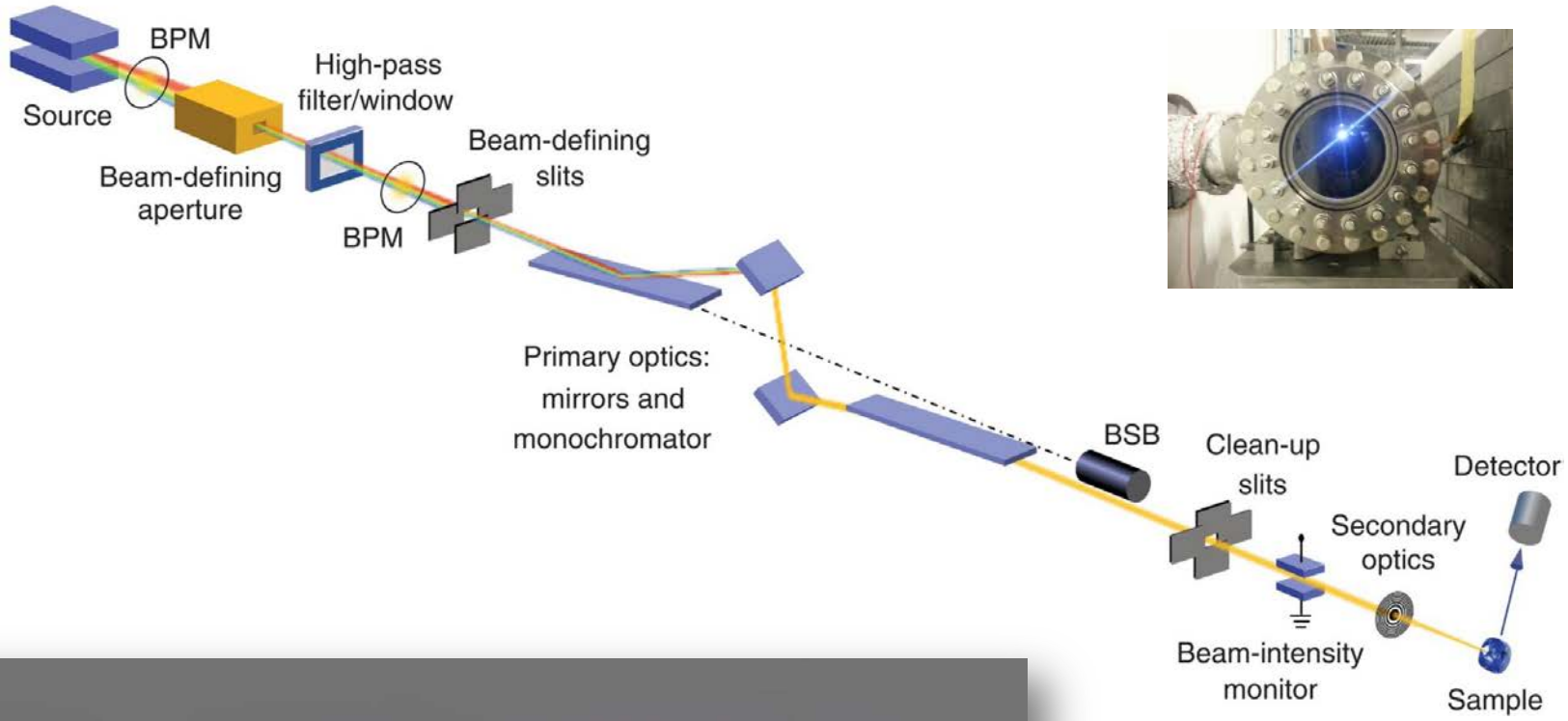

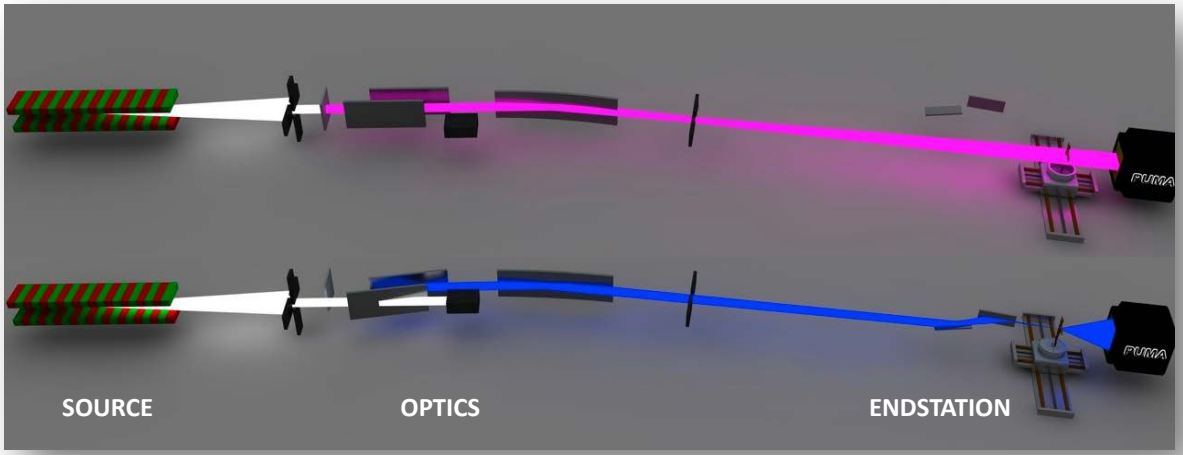

http://www.synchrotron-soleil.fr/Recherche/IPANEMA/methodessynchrotron

Seeing (through…) is believing!

Markus Raetz, Art Basel 2010

Representation of the beliefs in Ain Ghazal (Neolithic village), Jordan (6500 BCE)

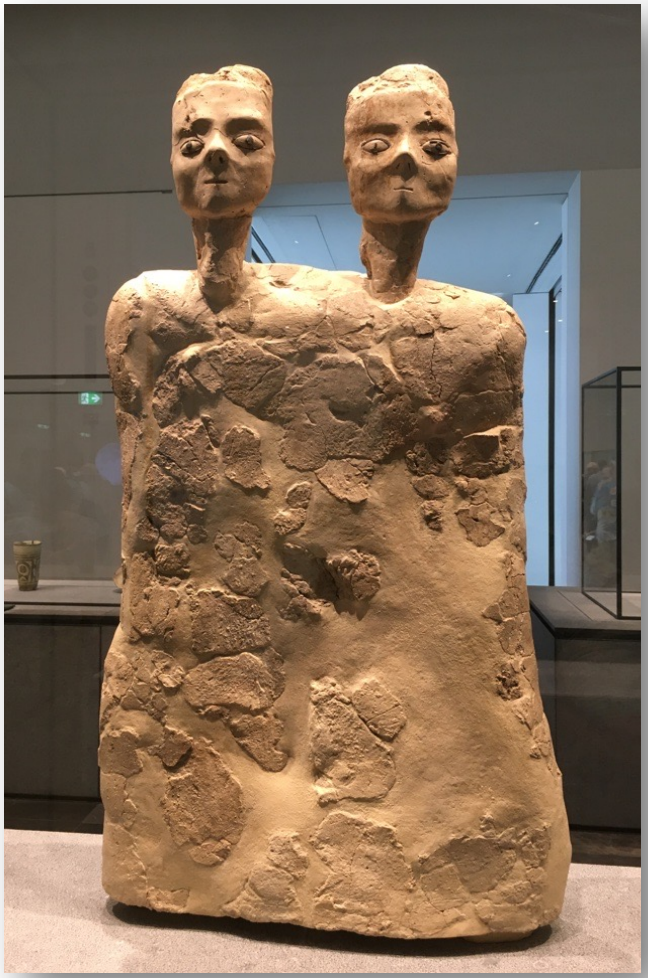

Louvre Abu Dhabi

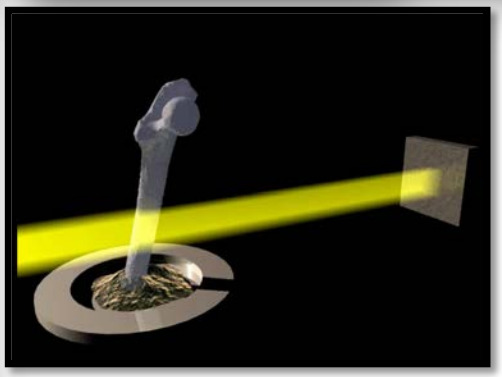

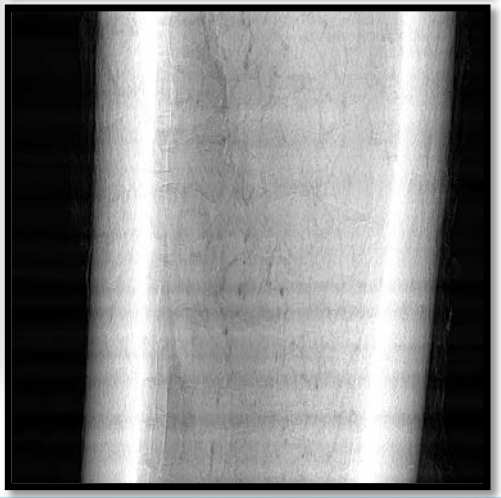

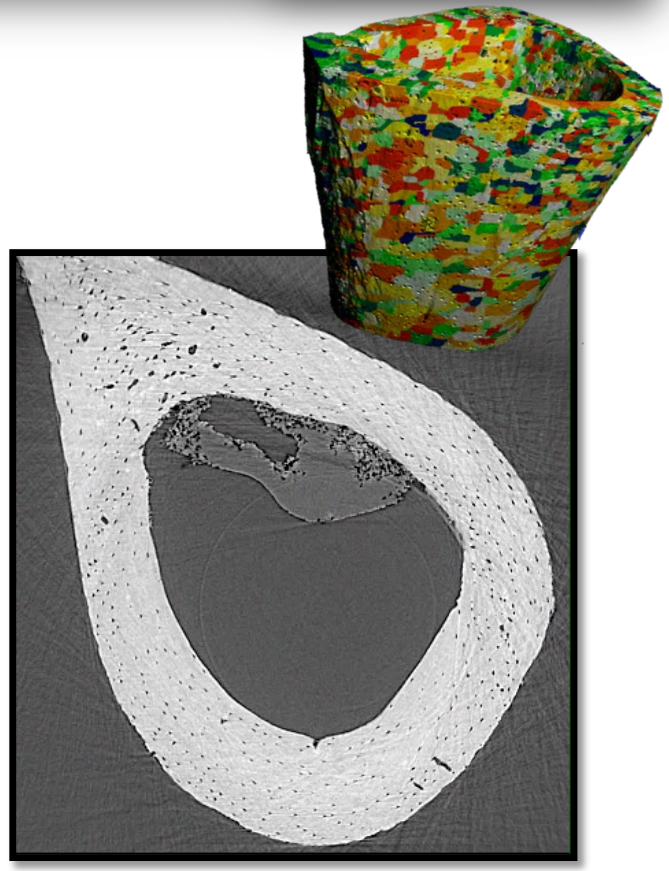

Behind the curtains of tomographic DAQ

https://youtu.be/TbLaQo3rgEE

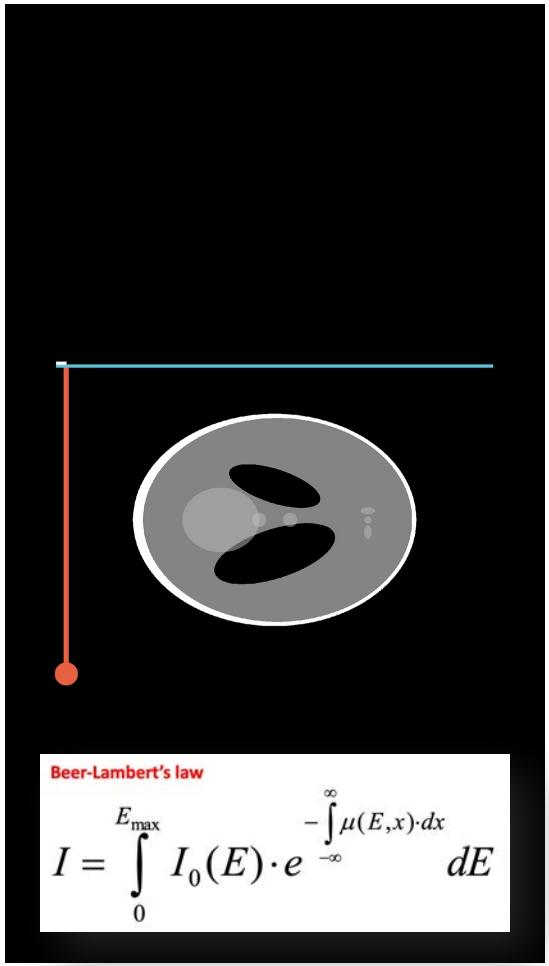

https://youtu.be/5Vyc1TzmNI8

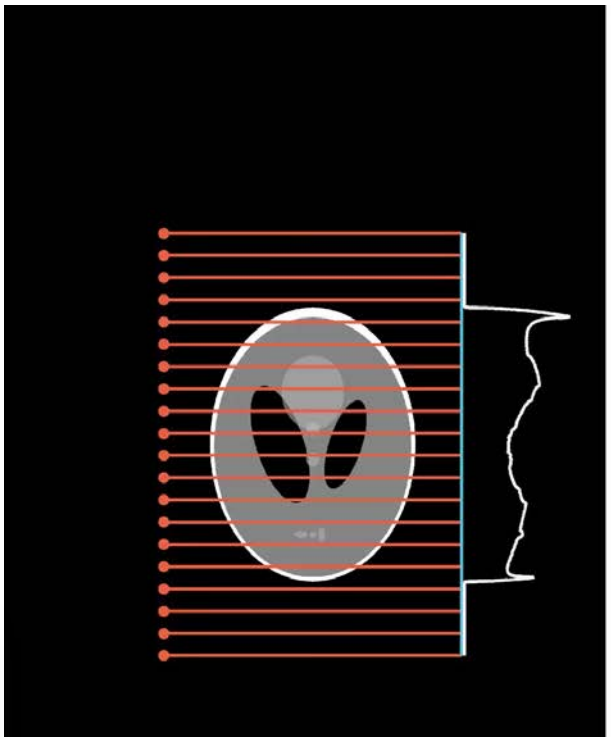

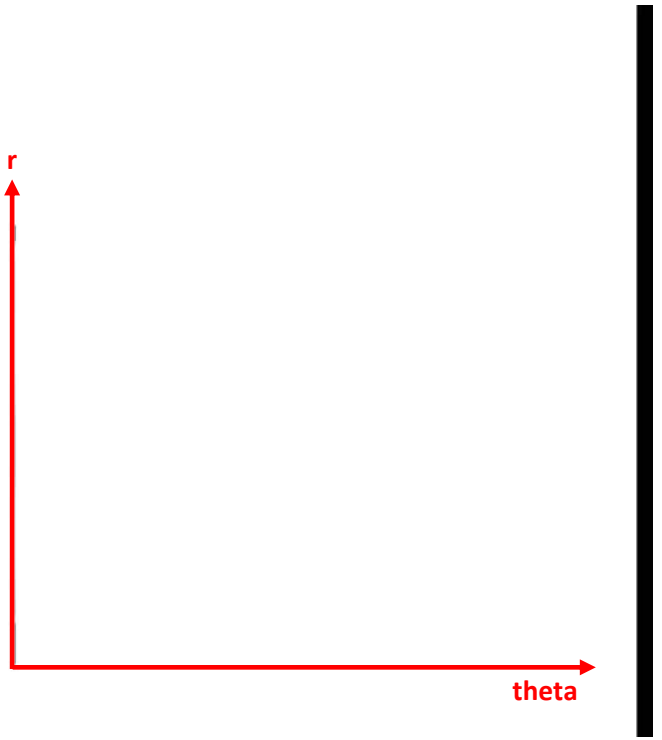

$$P = ln\frac{I_0}{I} = \int_0^d \mu(z)dz$$

Radon Transform, i.e. integral of a function over a (straight) line…

Tomographic reconstruction “at work”

Fourier Slice Theorem

The Fourier transform of a parallel projection of an object f(x,y) obtained at an angle θ equals a line of the 2D Fourier transform of f(x,y) taken at the same angle.

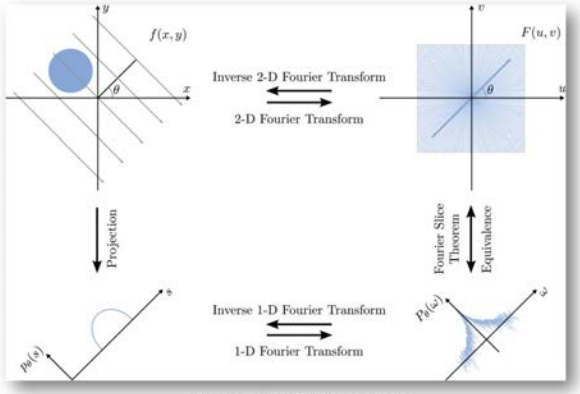

Figure from Meier et al., ISBN-13: 978-3-319-96519-2

FBP at work: demonstration

S. Siltanen - https://youtu.be/ddZeLNh9aac

$$\mu(x,y) = \int_0^{\pi} \mathrm{d}\theta \int_{-\infty}^{+\infty} \tilde{P}(\omega,\theta)|\omega| e^{j2\pi\omega t}\mathrm{d}\omega$$

https://youtu.be/ddZeLNh9aac

Filtered backprojection (math-background)

$$-\ln\left(\frac{I_\phi(r)}{I_0}\right) := P_\phi(r) = R(t,\phi) = \int_{-\infty}^{+\infty}\int_{-\infty}^{+\infty} \mu(x,y)\,\delta(x\cos\phi + y\sin\phi - t)\,dx\,dy$$

Image function

$$\mu(x,y) = \int_{-\infty}^{+\infty}\int_{-\infty}^{+\infty} \tilde{M}(u,\nu) e^{j2\pi(ux+\nu y)}\mathrm{d}u\mathrm{d}\nu$$

Coordinate transform (cartesian to polar)

$$\mu(x,y) = \int_0^{2\pi}\mathrm{d}\theta\int_0^{+\infty} \tilde{M}(\omega\cos\theta,\omega\sin\theta) e^{j2\pi\omega(x\cos\theta+y\sin\theta)}|g|\mathrm{d}\omega$$

Fourier Slice Theorem!

with $\begin{cases} u = \omega\cos\theta \\ \nu = \omega\sin\theta \end{cases}$ and $g = \begin{pmatrix} \frac{\partial u}{\partial\omega} & \frac{\partial u}{\partial\theta} \\ \frac{\partial\nu}{\partial\omega} & \frac{\partial\nu}{\partial\theta} \end{pmatrix} = \begin{pmatrix} \cos\theta & -\omega\sin\theta \\ \sin\theta & \omega\cos\theta \end{pmatrix}$

$$\mu(x,y) = \int_0^{2\pi}\mathrm{d}\theta\int_0^{+\infty} \tilde{P}(\omega,\theta) e^{j2\pi\omega(x\cos\theta+y\sin\theta)}\omega\mathrm{d}\omega$$

Symmetry properties $\tilde{P}(\omega,\theta+\pi) = \tilde{P}(-\omega,\theta)$

Image function: $\mu(x,y) = \int_0^{\pi}\mathrm{d}\theta\int_{-\infty}^{+\infty} \tilde{P}(\omega,\theta)|\omega| e^{j2\pi\omega t}\mathrm{d}\omega$

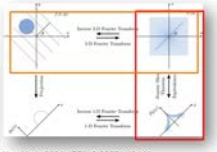

A. C. Kak, M. Slaney, Principle of Computerized Tomographic Imaging", SIAM Classics in Applied Mathematics 33, New York, 2001, ISBN 0-89871-494-X

Full-field microscopy (zone plates)

(50-500 nm resolution)

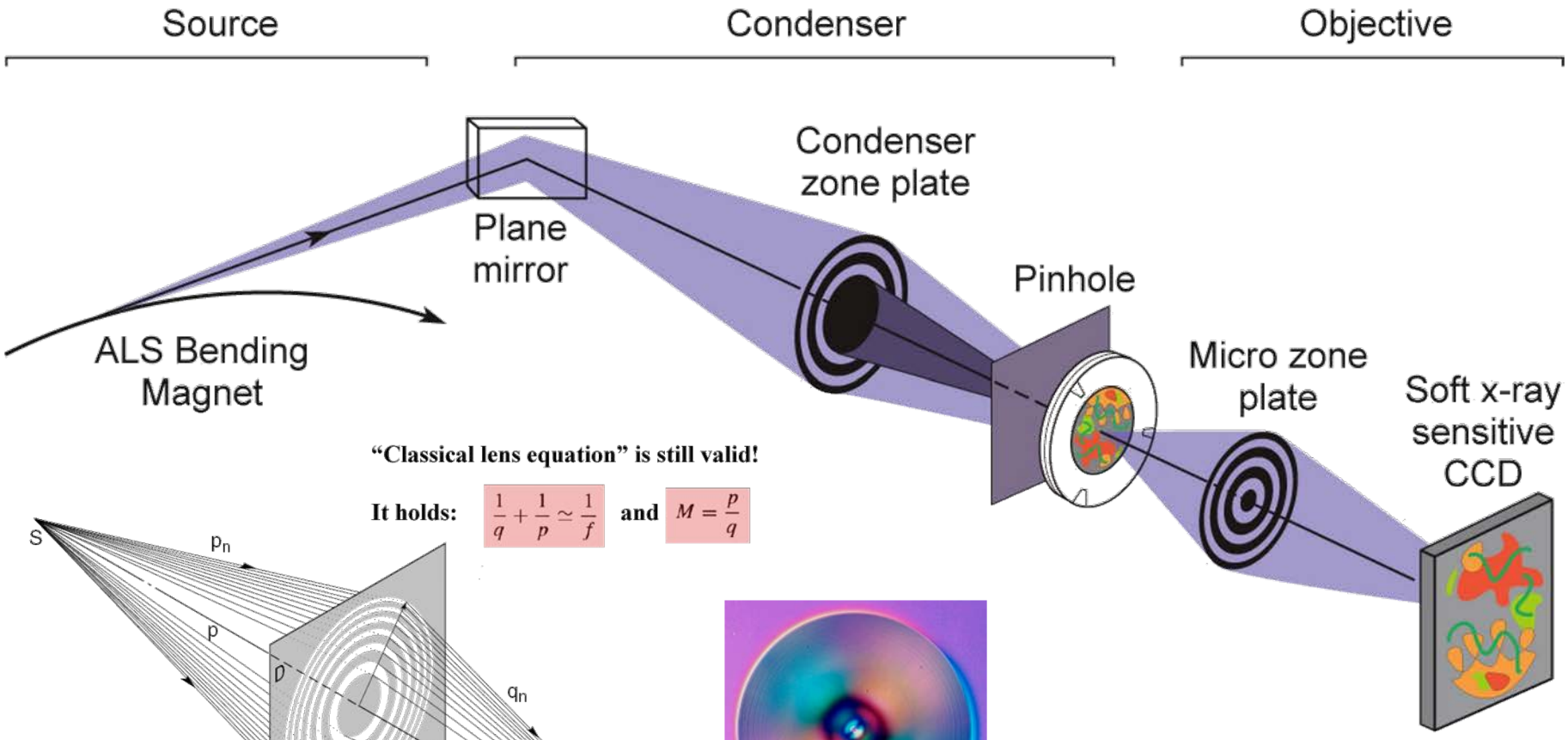

"Classical lens equation" is still valid!

It holds: $\frac{1}{q}+\frac{1}{p}\simeq\frac{1}{f}$ **and** $M=\frac{p}{q}$

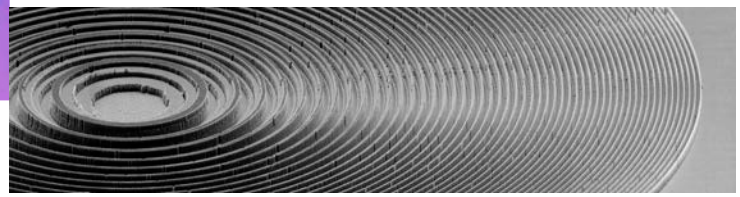

Images courtesy of D. Attwood (UC Berkeley) and C. David (PSI)

Cryo full-field tomographic (absorption) microscopy

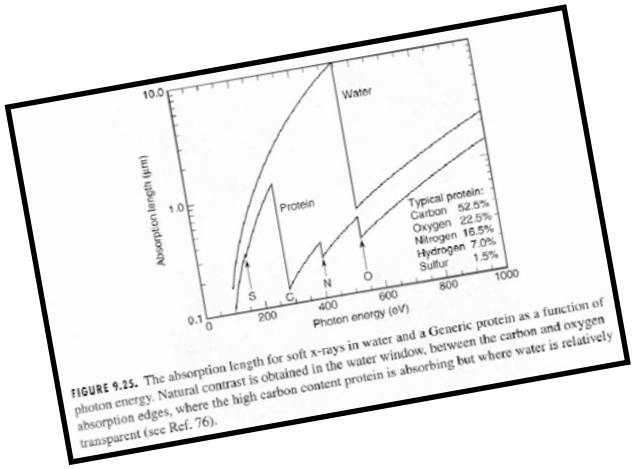

FIGURE 9.25. The absorption length for soft x-rays in water and a Generic protein as a function of photon energy. Natural contrast is obtained in the water window, between the carbon and oxygen absorption edges, where the high carbon content protein is absorbing but where water is relatively transparent (see Ref. 76).

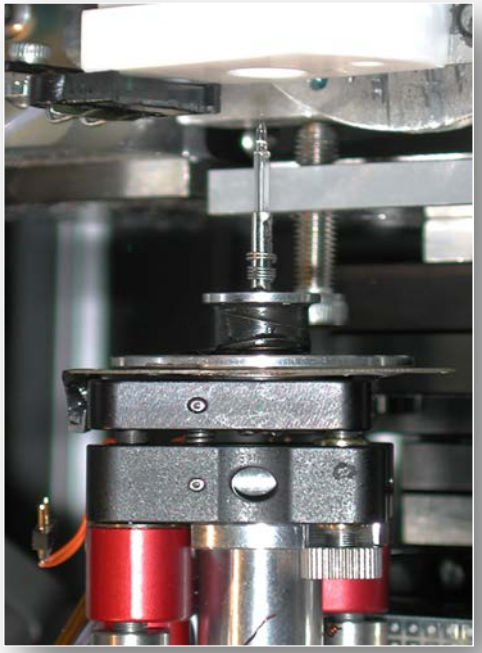

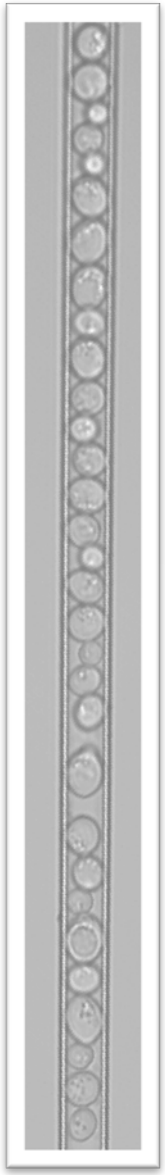

Projection images

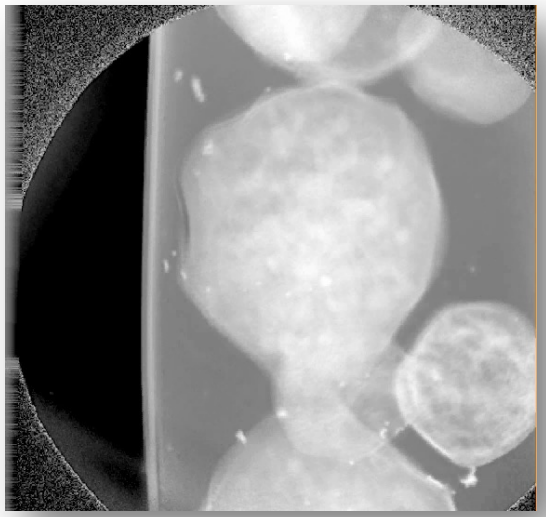

Saccharomyces cerevisiae
(yeast cells)

Sagittal orthoslicing

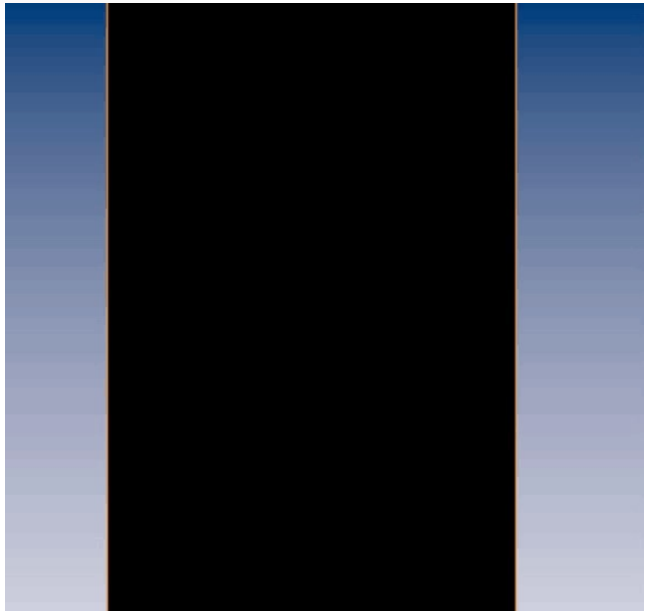

C.A. Larabell & M. A. Le Gros
Molecular Biology of the Cell 15(3), 956-962 (2004)

Full-field parallel projection imaging

(1-50 microns)

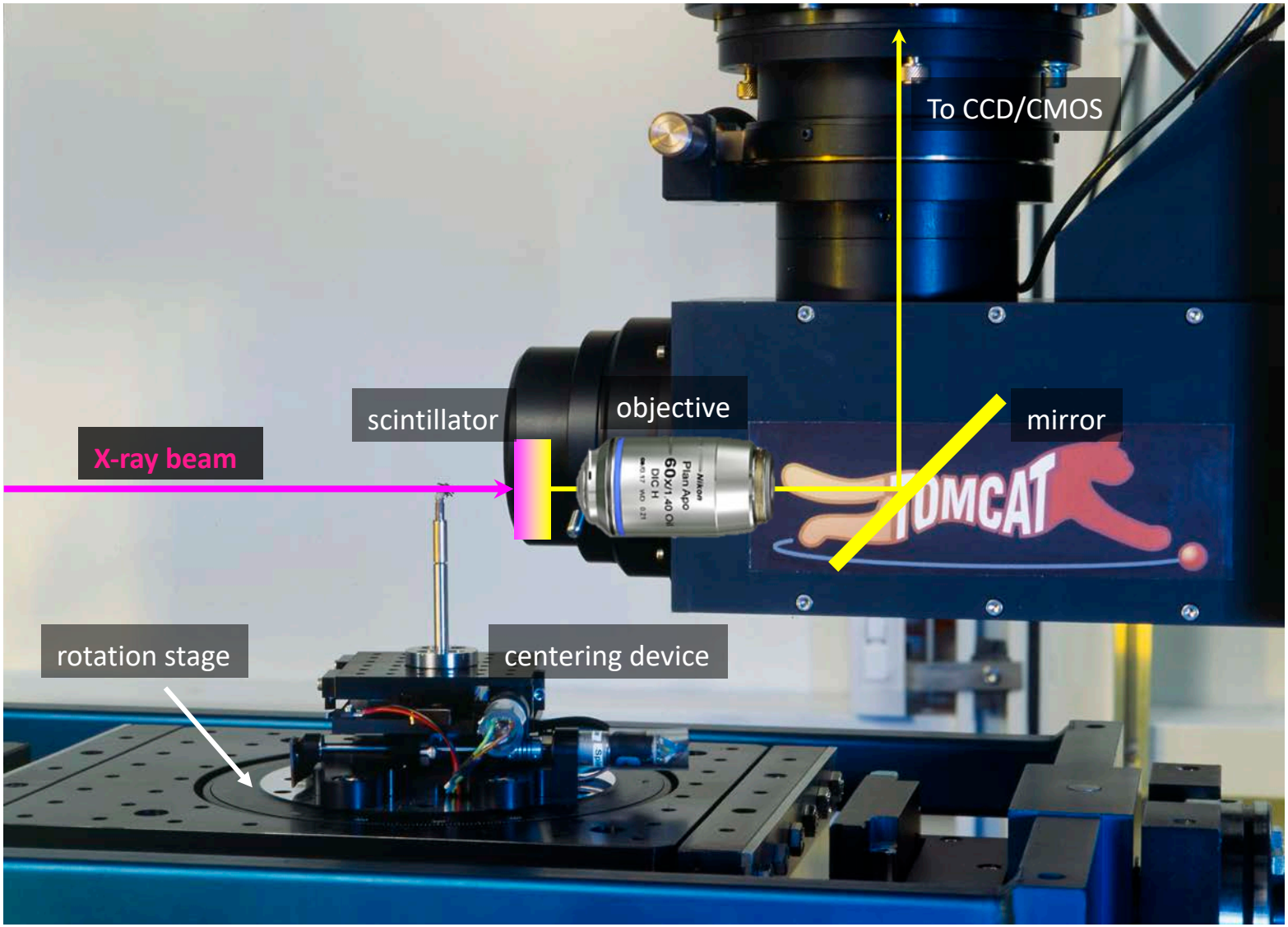

The first predator on earth: 500 Myears ago

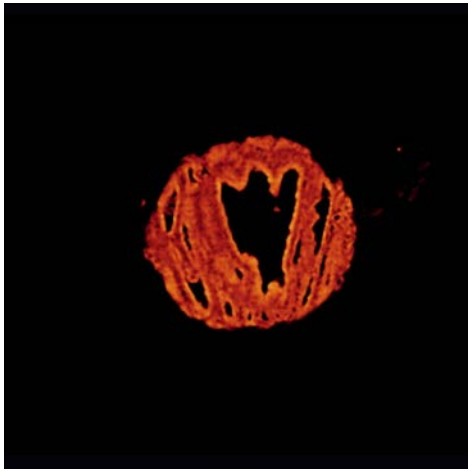

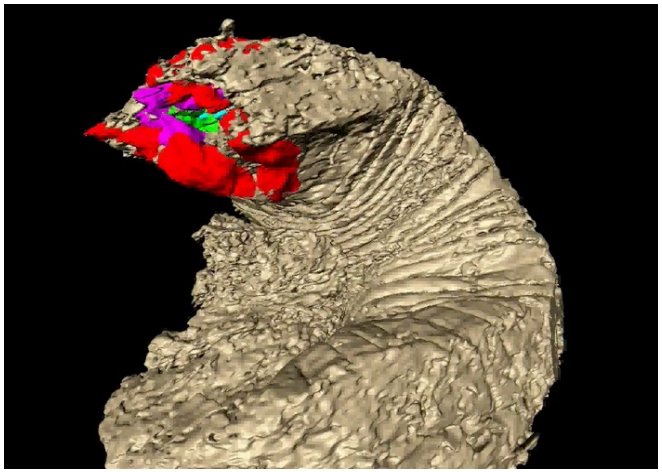

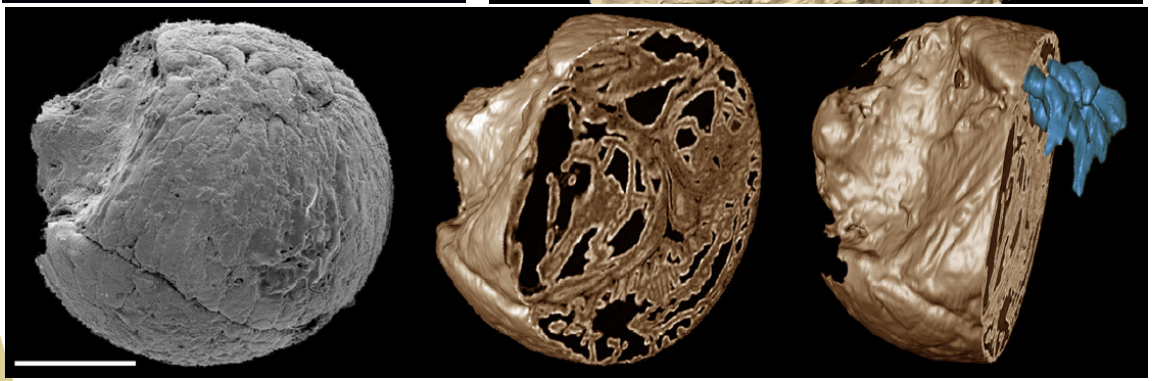

P. Donoghue, M. Stampanoni et al., Nature 442 (2006)

In-situ :: Operando :: In-vivo :: In-fieri

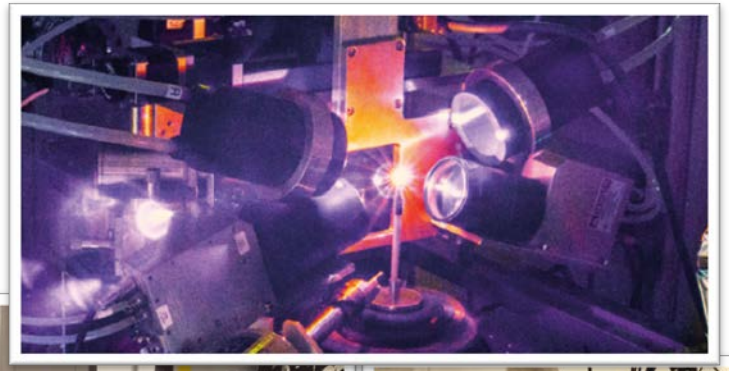


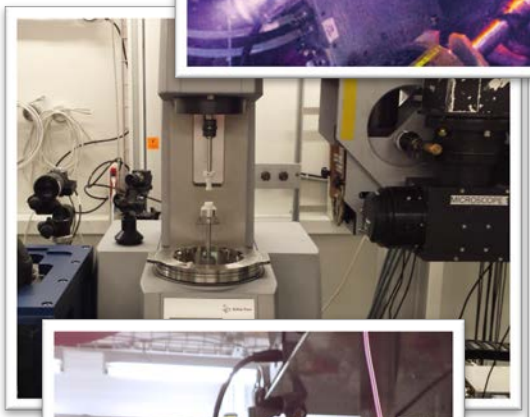
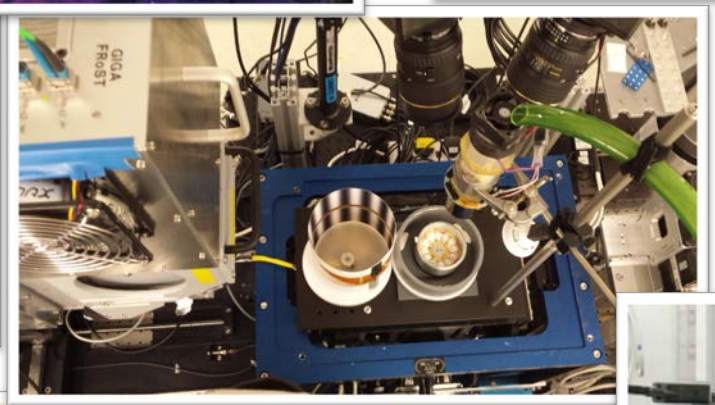
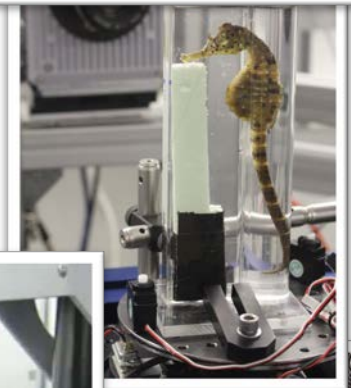

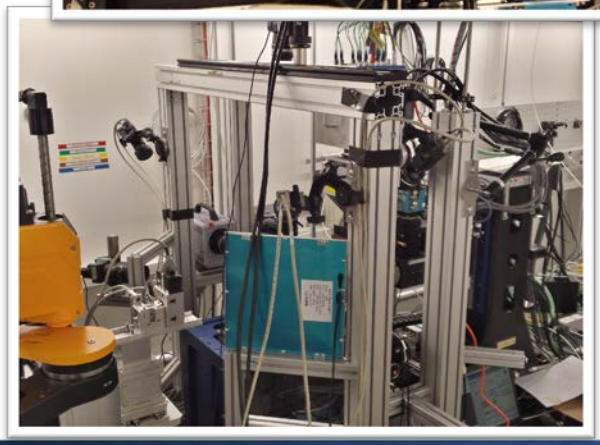
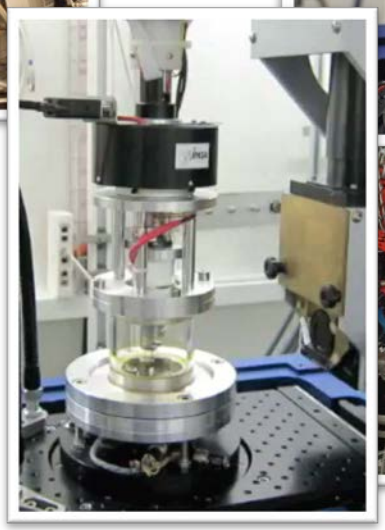
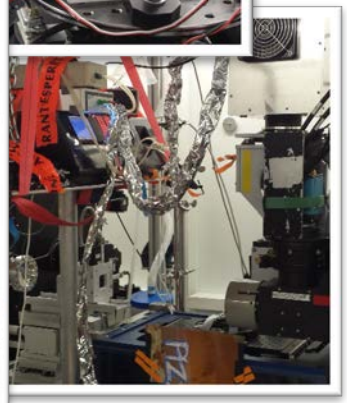

«Chasing the phase…»

General form of a wave in vacuum: $\psi_{vacuum}(\vec{r},t) = Ae^{i(\vec{k}\cdot\vec{r}-\omega t)}$

For a wave traveling in the z-direction: $\vec{k} = (0,0,k = \frac{2\pi}{\lambda})$

Plane wave propagating in z-direction: $\psi_{vacuum}(\vec{r},t) = Ae^{i(\vec{k}\cdot\vec{r}-\omega t)} = Ae^{i(kz-\omega t)}$

For a wave traveling in a medium: $n = 1 - \boldsymbol{\delta} + i\boldsymbol{\beta}$

Wave propagating in a medium: $\psi_{medium}(z,t) = Ae^{i(nkz-\omega t)} = Ae^{-i\omega t}e^{(1-\delta)ikz}e^{-\beta kz} =$

$= \psi_{vacuum} \cdot e^{-i\delta kz} \cdot e^{-\beta kz}$

Phase-shift Attenuation

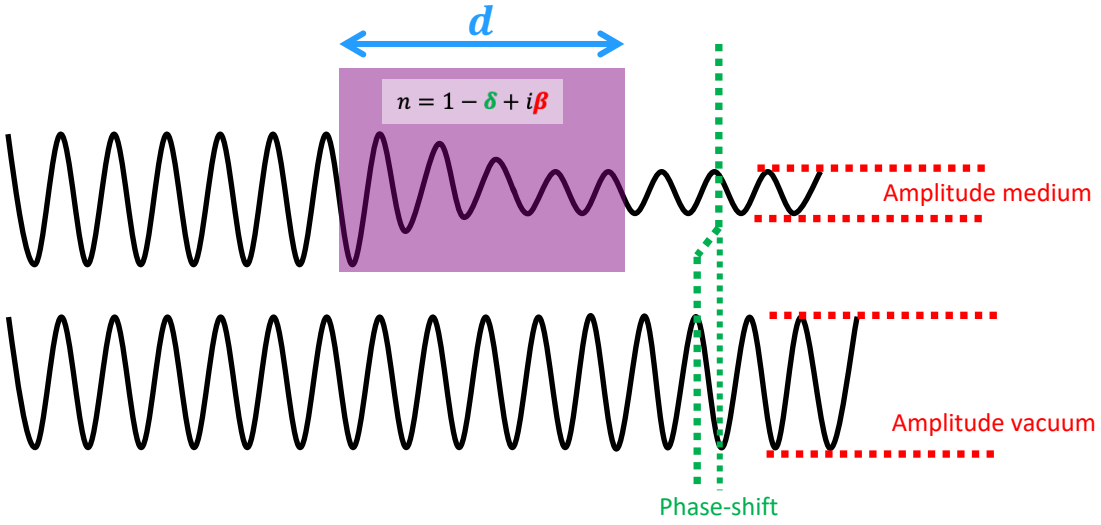

After medium of length d:

$$\boldsymbol{T(d)} = \frac{I_m(d)}{I_v(0)} = \frac{|\psi_m(d,t)|^2}{|\psi_v(0,t)|^2} = e^{-2k\beta d}$$

$$\boldsymbol{\Delta\phi(d)} = \delta kd$$

Why is phase contrast so interesting?

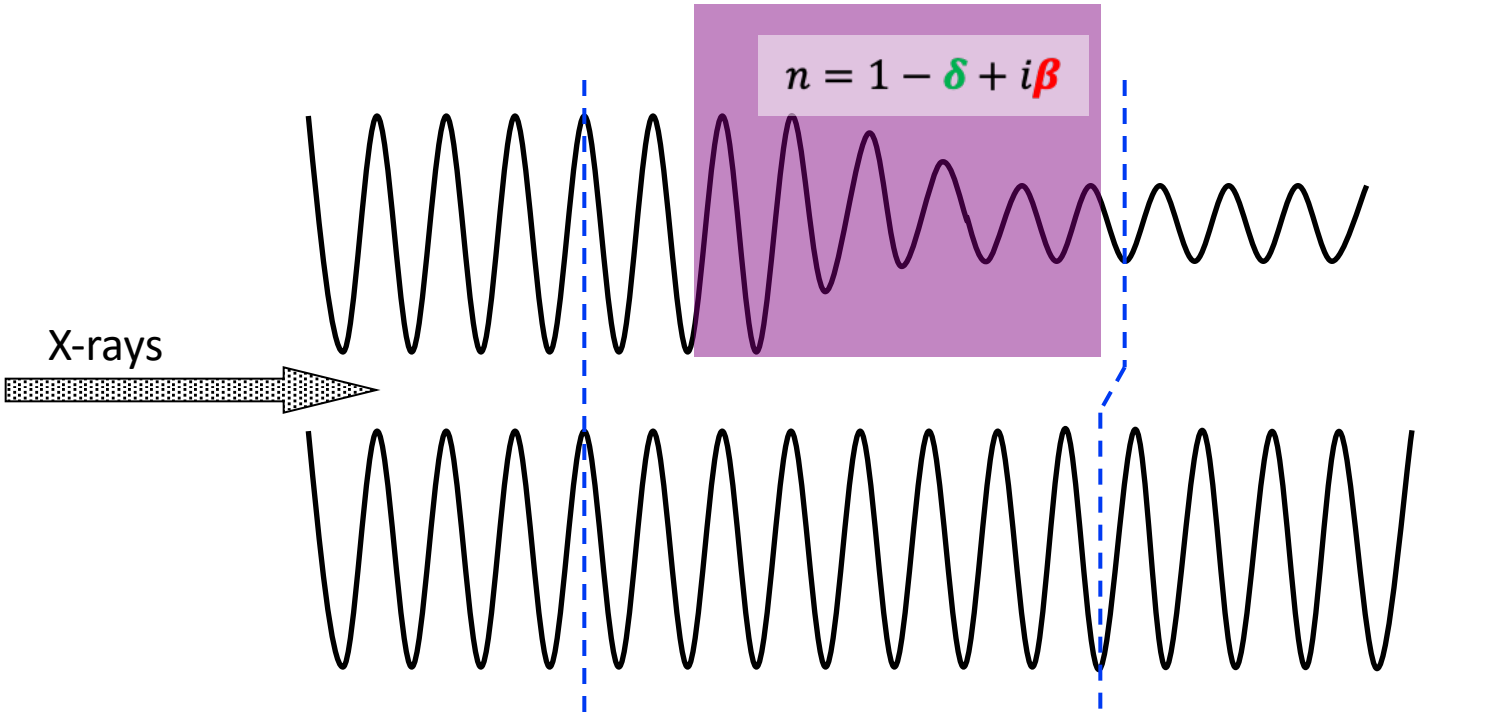

Example:

- 20 keV x-rays
- Organic sample (polymer, biological, medical…)
- 50 µm thickness

➔ **only 0.2 % absorption**

➔ **but π phase shift!!**

- **Higher contrast !!**
- **Lower dose**

Phase vs absorption CT

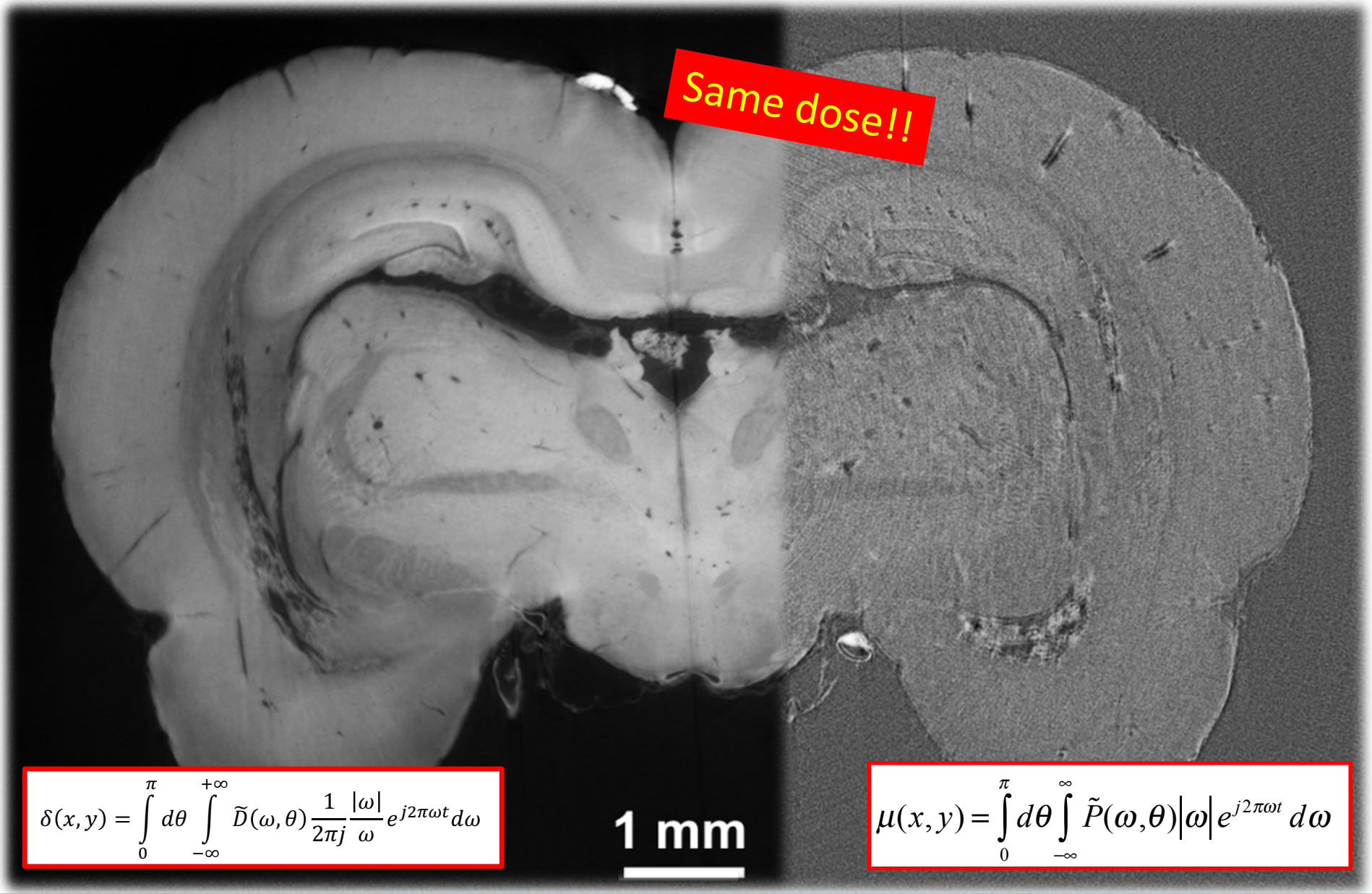

$$\delta(x,y) = \int_0^{\pi} d\theta \int_{-\infty}^{+\infty} \tilde{D}(\omega,\theta) \frac{1}{2\pi j} \frac{|\omega|}{\omega} e^{j2\pi\omega t} d\omega$$

$$\mu(x,y) = \int_0^{\pi} d\theta \int_{-\infty}^{\infty} \tilde{P}(\omega,\theta) |\omega| e^{j2\pi\omega t} d\omega$$

X-ray phase contrast techniques

$\Phi(x,y)$

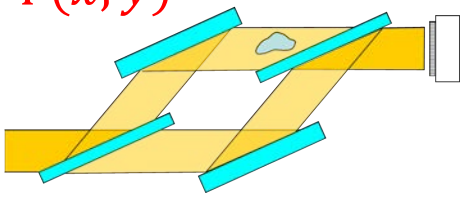

Crystal interferometry
Bonse et al. APL 6, 155 (1965)

$\frac{\partial}{\partial y}\Phi(x,y)$

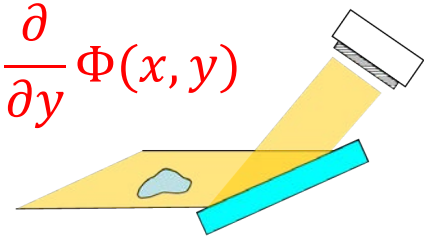

Analyser-based (DEI)
Chapman et al., *PMB,* 42, 2015 (1997)
Davis et al., JOSA A 13, 1193 (1996)

$\frac{\partial^2}{\partial y^2}\Phi(x,y)$

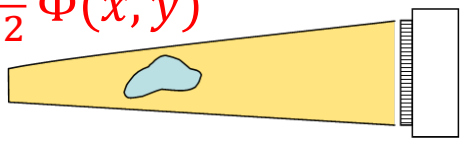

Free Space Propagation (TIE)
Snigirev et al., RSI 66, 5486 (1995)
Cloetens et al., APL 75, 2912 (1999)
Groso et al., OptExp 14, 8103 (2006)

$\Phi(x,y)$

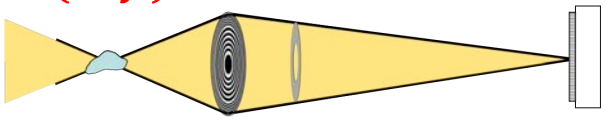

Zernike Phase Contrast
Weiss et al., UM 84, 185 (2000)
Stampanoni et al., PRB 81, 140105R (2010)

$\frac{\partial}{\partial y}\Phi(x,y)$

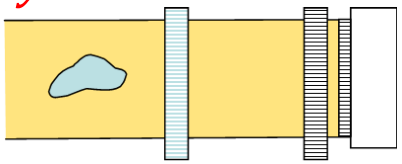

Grating interferometry (DPC)
Weitkamp et al., OptExp 13, 6296 (2005)
Pfeiffer et al., Nature Phys 2, 258 (2006)

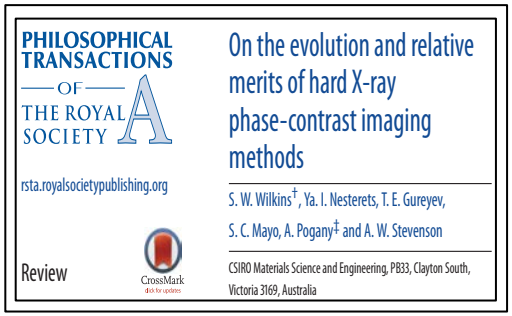

$\Phi(x,y)$

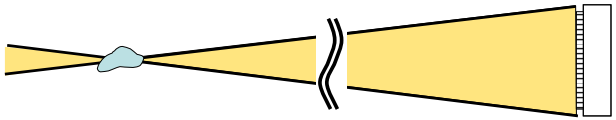

Coherent Diffraction Imaging (CDI)
Miao et al., Nature 400 (1999)
Thibault et al., Science, 321, 379 (2008)

Coded apertures
Olivo, APL 91 (7) 2007

Zernike (full-field) phase contrast microscopy

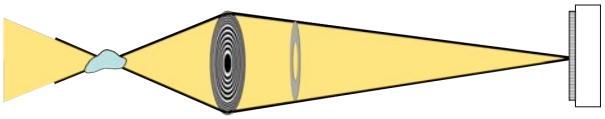

Zernike Phase Contrast
Weiss et al., UM 84, 185 (2000)
Stampanoni et al., PRB 81, 140105R (2010)

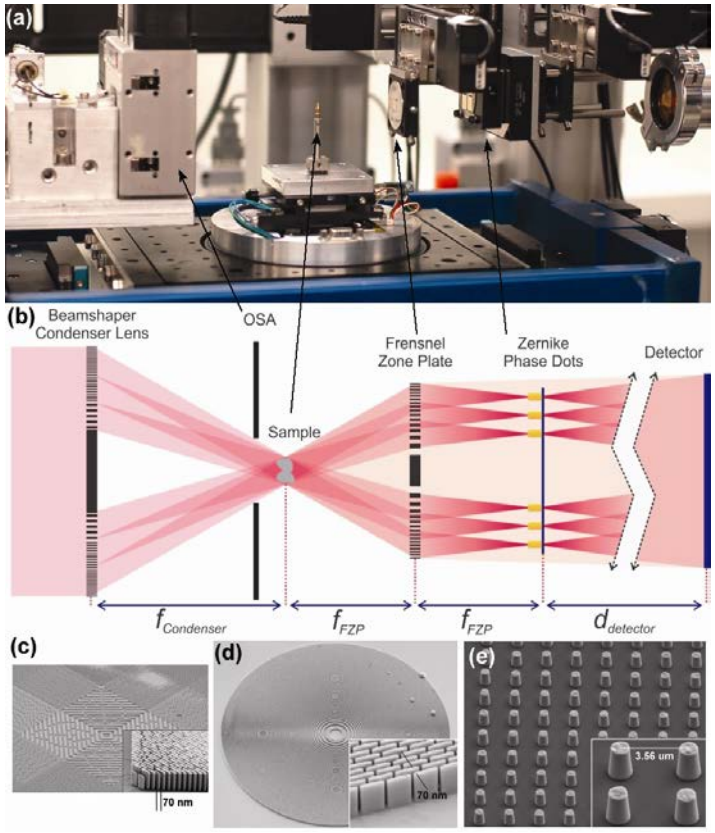

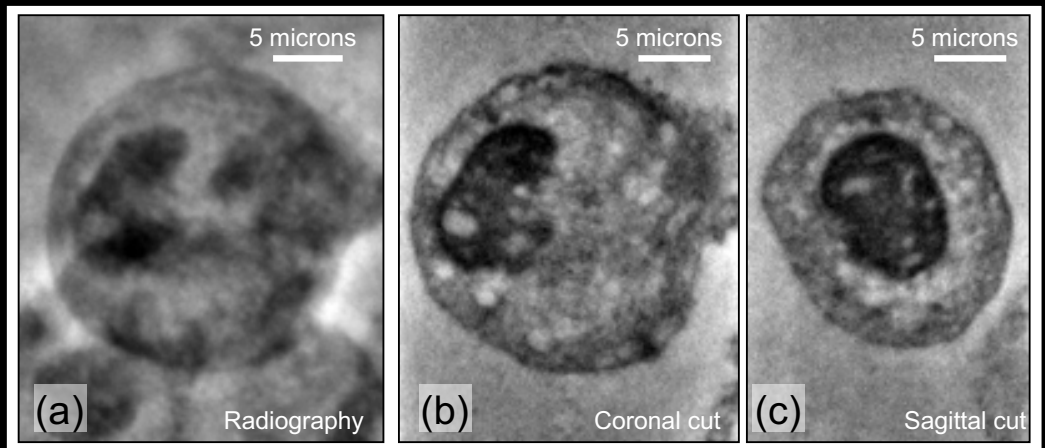

Nanotomography of
MC3 preosteoblast cells
@TOMCAT

- 10 keV (!)
- Pixel size: 70 nm
- True 3D res: ~ 200 nm
- High penetration power !
- High depth of focus !

Holotomography and Cryo-ptychography

(phase contrast bioimaging at the nanoscale)

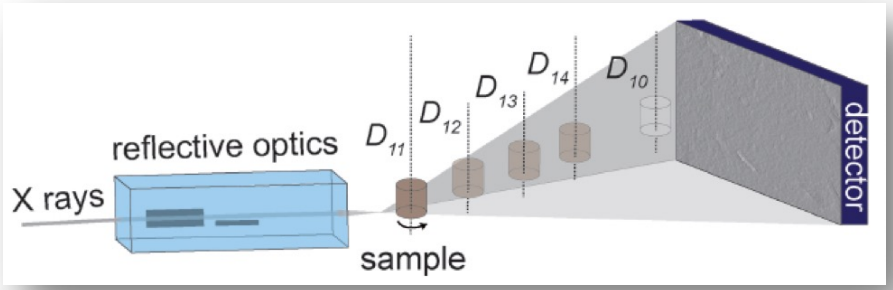

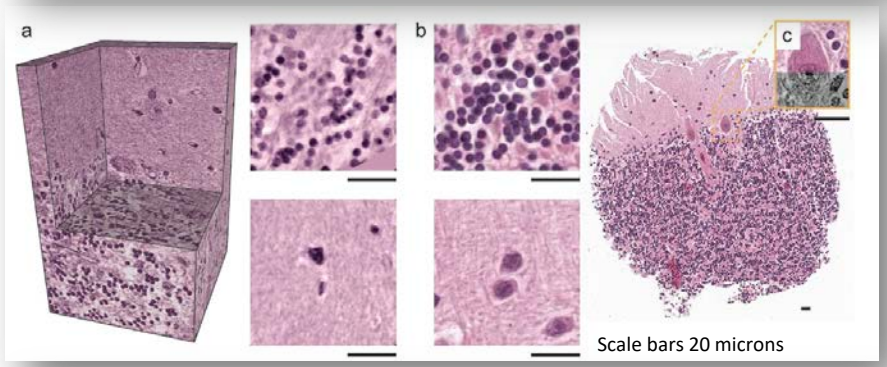

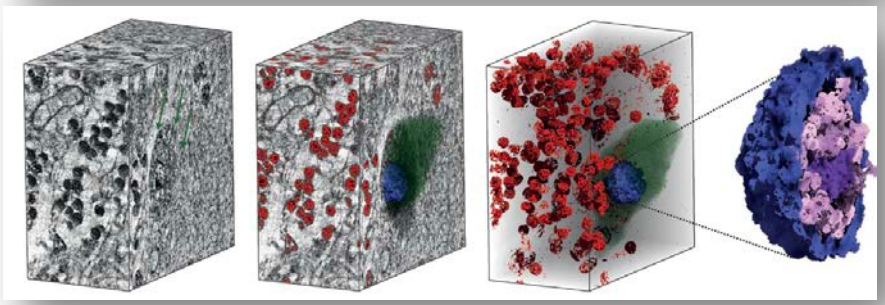

A 3D rendering of (sub)cellular structures within a Purkinje cell: cell soma (green), nuclear envelope (blue), nuclear content (pink), and nucleolus (violet), granule cell nuclei (red). Average diameter of Purkinje cell soma: 54 µm; average diameter of Purkinje cell nucleolus 3.5 µm. ***Kimchenko et al, Advanced Science, 2018***

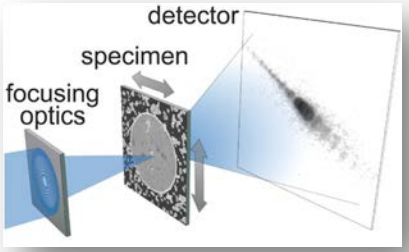

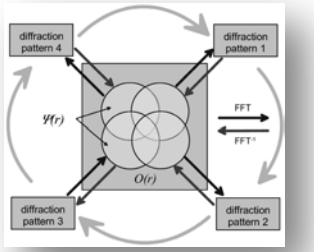

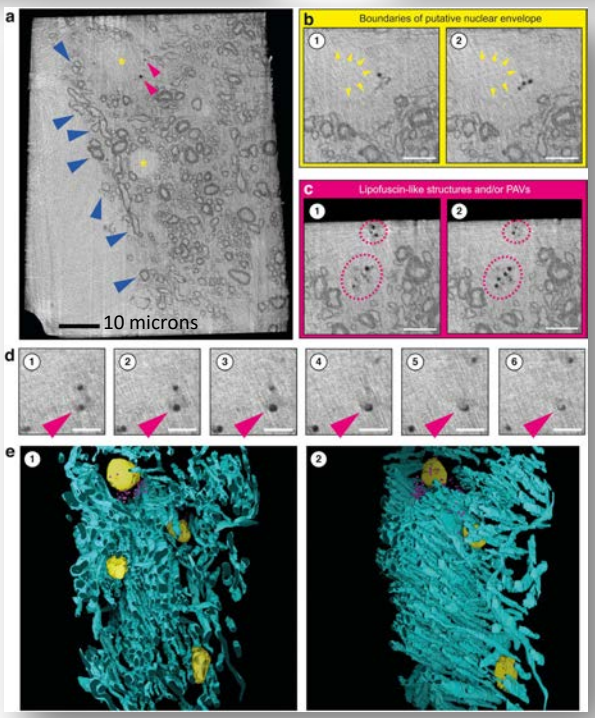

Variations of myelin sheath thicknesses of myelinated axons (dark blue arrowheads). Multiple cell nuclei (yellow asterisks) are detected based on size, and contrast differences to the surrounding cellular cytosol. Tomo: Yellow = nuclei, Pink = lysosomal LF, Aqua = Myelinated axons. ***Shahmoradian et al, Scientific Reports 2017***

Free-space propagation phase contrast imaging

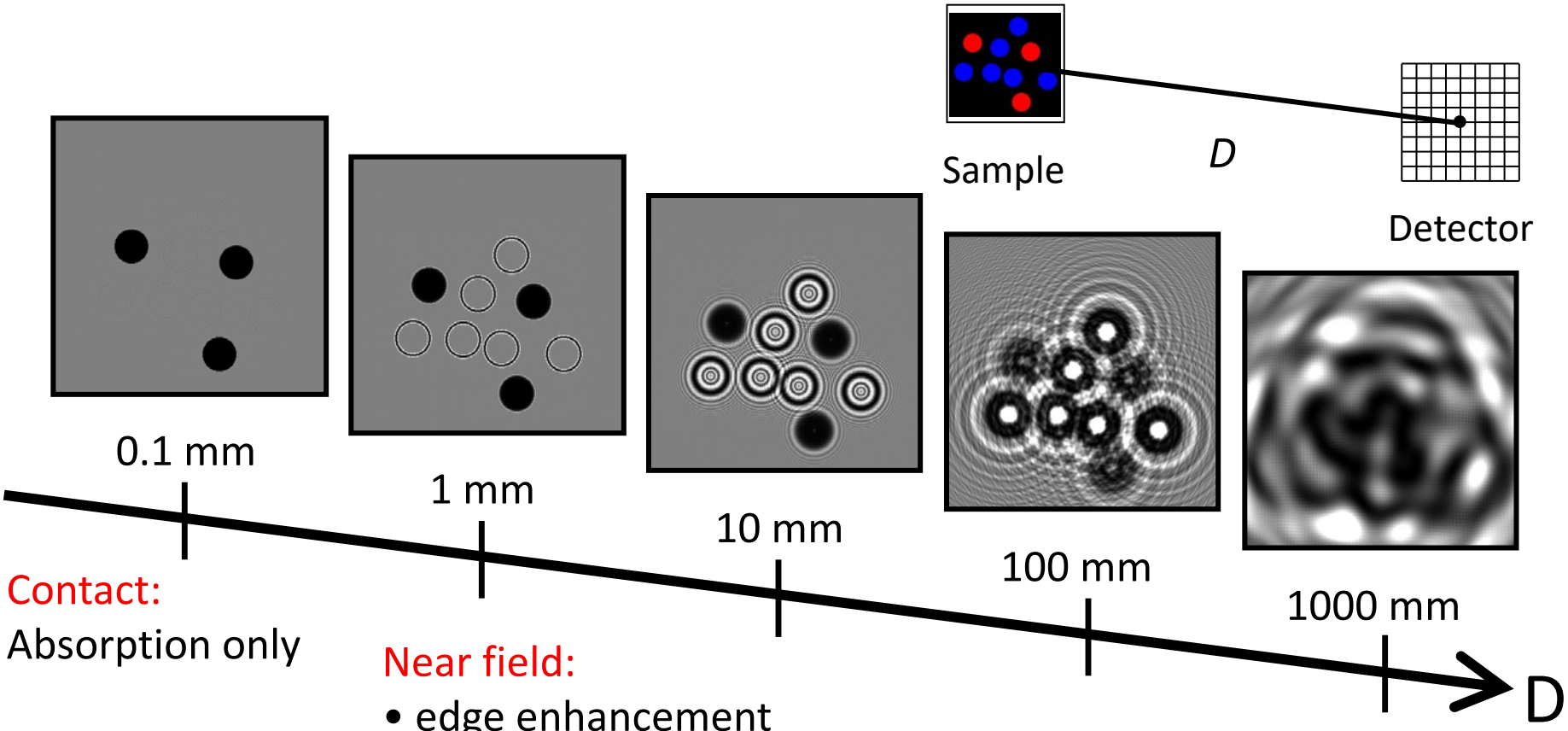

Contact:
Absorption only

Near field:
- edge enhancement
- phase objects detectable

Far field:
- Coherent Diffraction Img.

$$H(\nu_x, \nu_y) = \exp\left[-i2\pi\sqrt{\frac{1}{\lambda^2} - \nu_x^2 - \nu_y^2}\cdot d\right]$$

Transfer function of the free space → Phase factor builds up!

Free-space propagation phase contrast…"at work"

Cörek et al, Small, Volume: 16, Issue: 31, First published: 22 June 2020, DOI: (10.1002/smll.202000746)

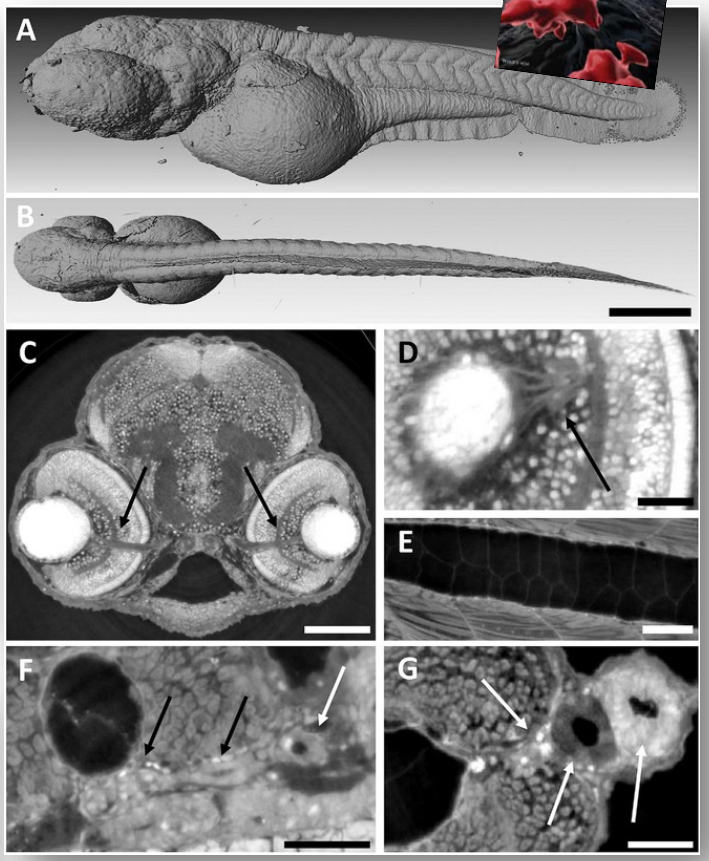

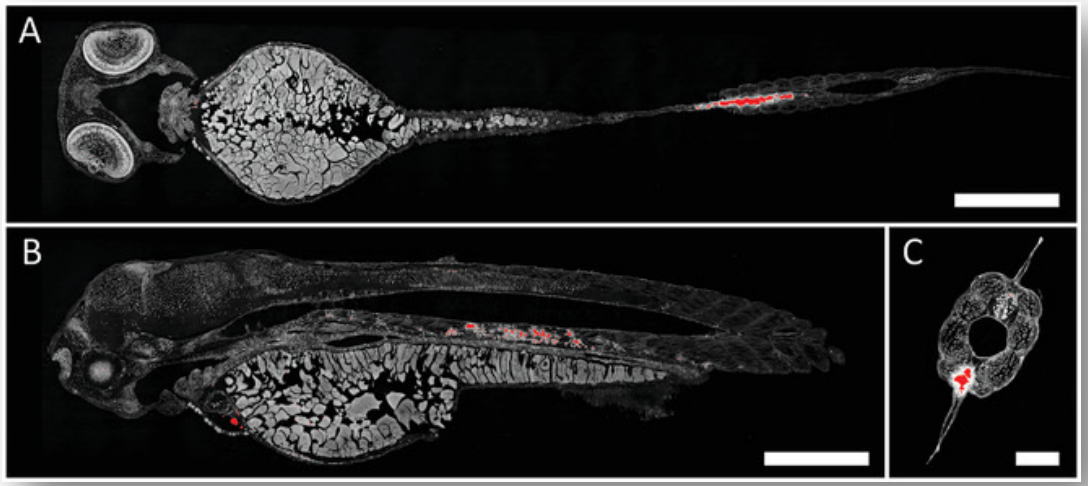

3D surface rendering and virtual histology of the zebrafish embryo from SRμCT. 3D surface rendering in A) lateral direction and B) dorsal-ventral direction of a 48 hpf zebrafish embryo. C) Virtual tissue sections showing the brain and the eyes of the embryo (transverse plane through the head). The optic nerves are labeled with black arrows. D) Magnification of the eye showing the retina and optical nerve fenestrations (transverse plane, black arrow). E) Notochord with surrounding muscle fibers (midsagittal plane through the tail). F) Pronephron with glomerulus (sagittal plane, dorsal location next to the yolk sac, white arrow) and tubules (black arrows). G) Gut (transverse plane through the tail cranial to the cloaca, right arrow), kidney tubule (middle arrow), and the caudal vein (left arrow). Scale bars correspond to 200 μm (A,B); 70 μm (C,E); 20 μm (D,F,G).

Hunting the complete mouse brain microvascular architecture

This is a stitched tomogram of more than 1000 single volumes, assembled non-rigidly.
Size of data shown: 11 Tb

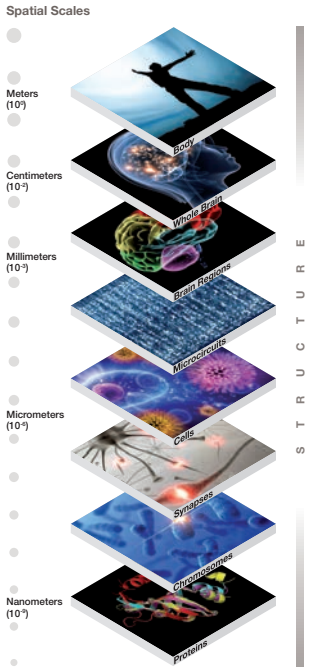

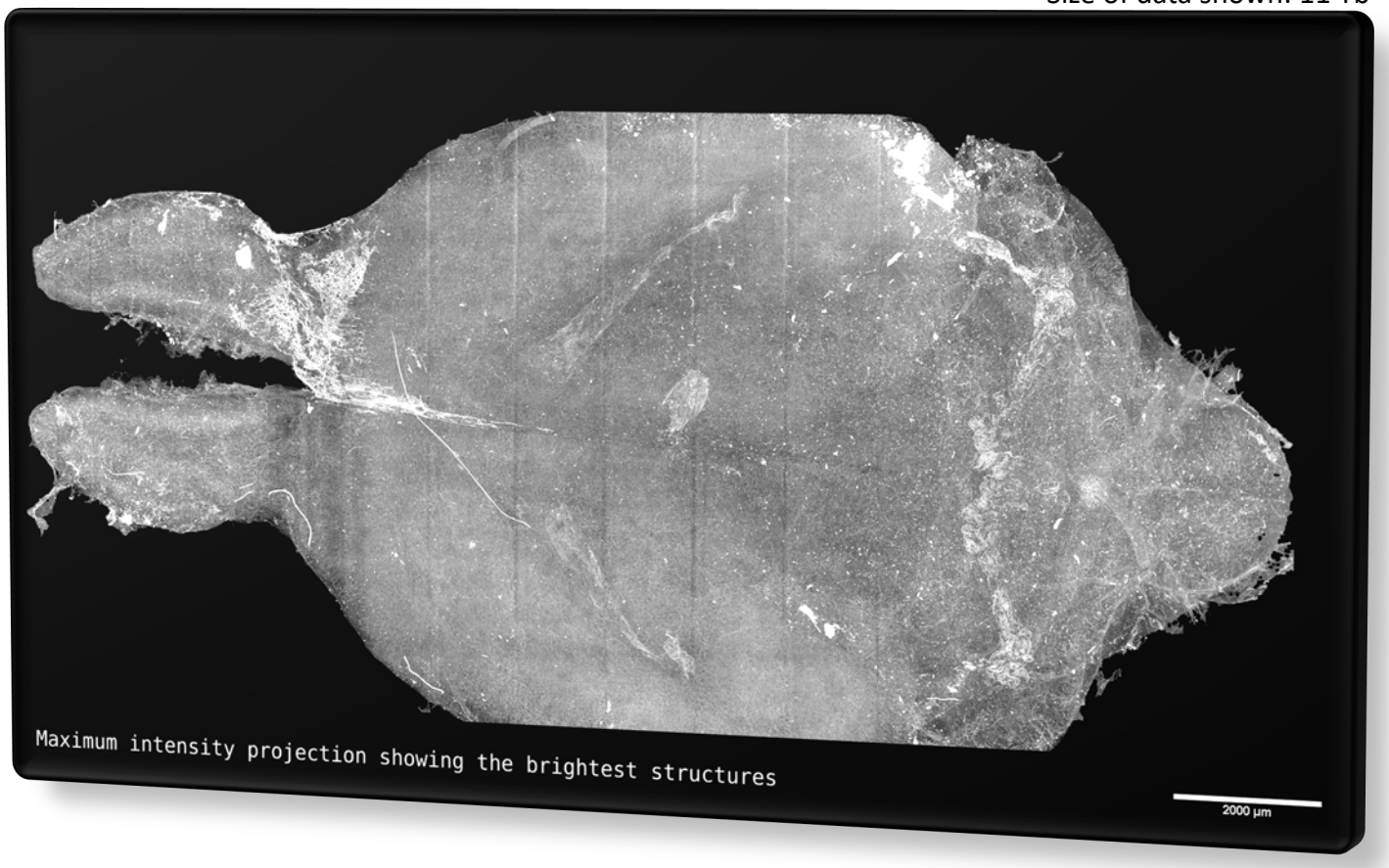

Human Brain Project

A. Miettinen, A. Bonnin, M. Stampanoni et al., BioInformatics 2019
T. Wälchi, M. Stampanoni et al., Nature Protocols 2021

Metal foams @ 1000 tps (tomograms per second)

World record!

Observe formation and coalescence of bubbles inside a metal foam during heating

Thixocast AlSi6Cu4 + 0.8 wt% TiH2 alloy

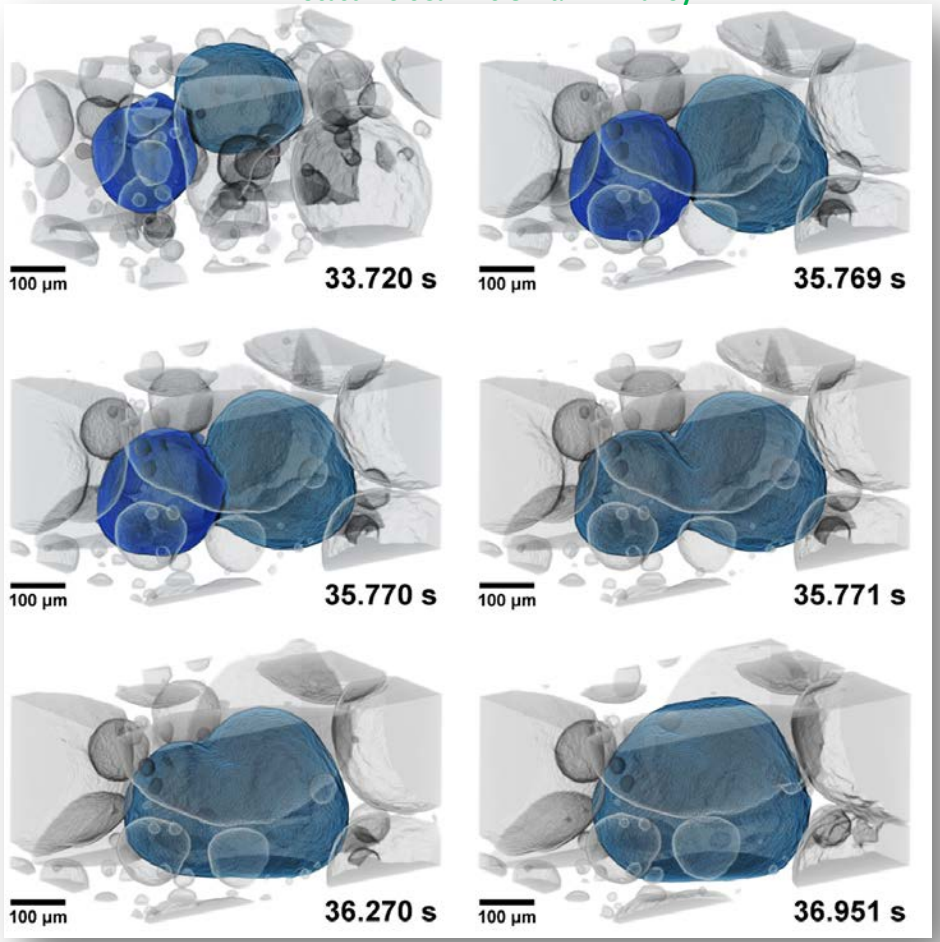

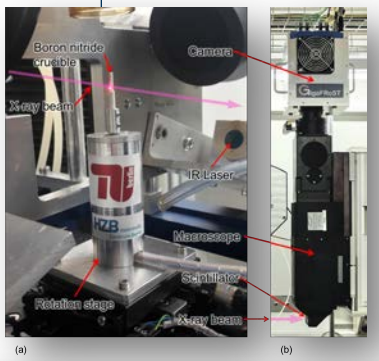

Real time

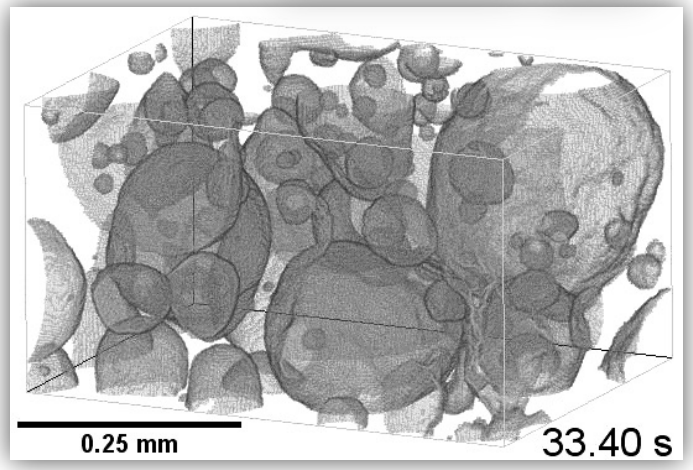

40x slower

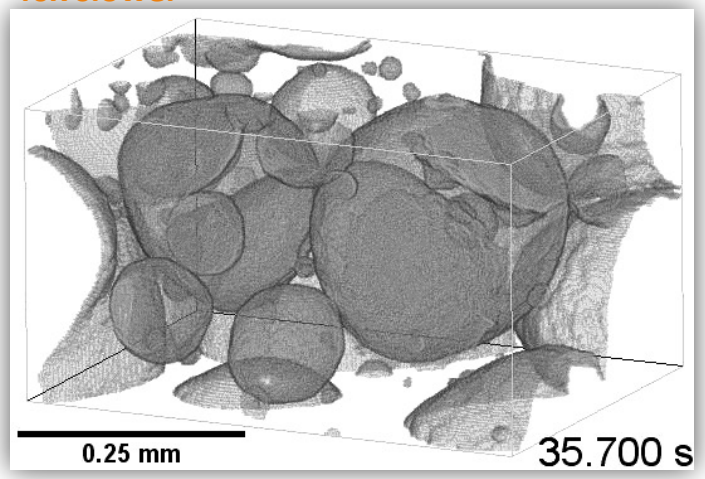

F. García-Moreno, C. Schlepütz et al., Advanced Materials, *in press*
Data available at: https://doi.org/10.16907/d7582cb6-7850-42bc-ad76-e845b998e9ca

Gratings (Talbot) interferometry: a very sensitive technique

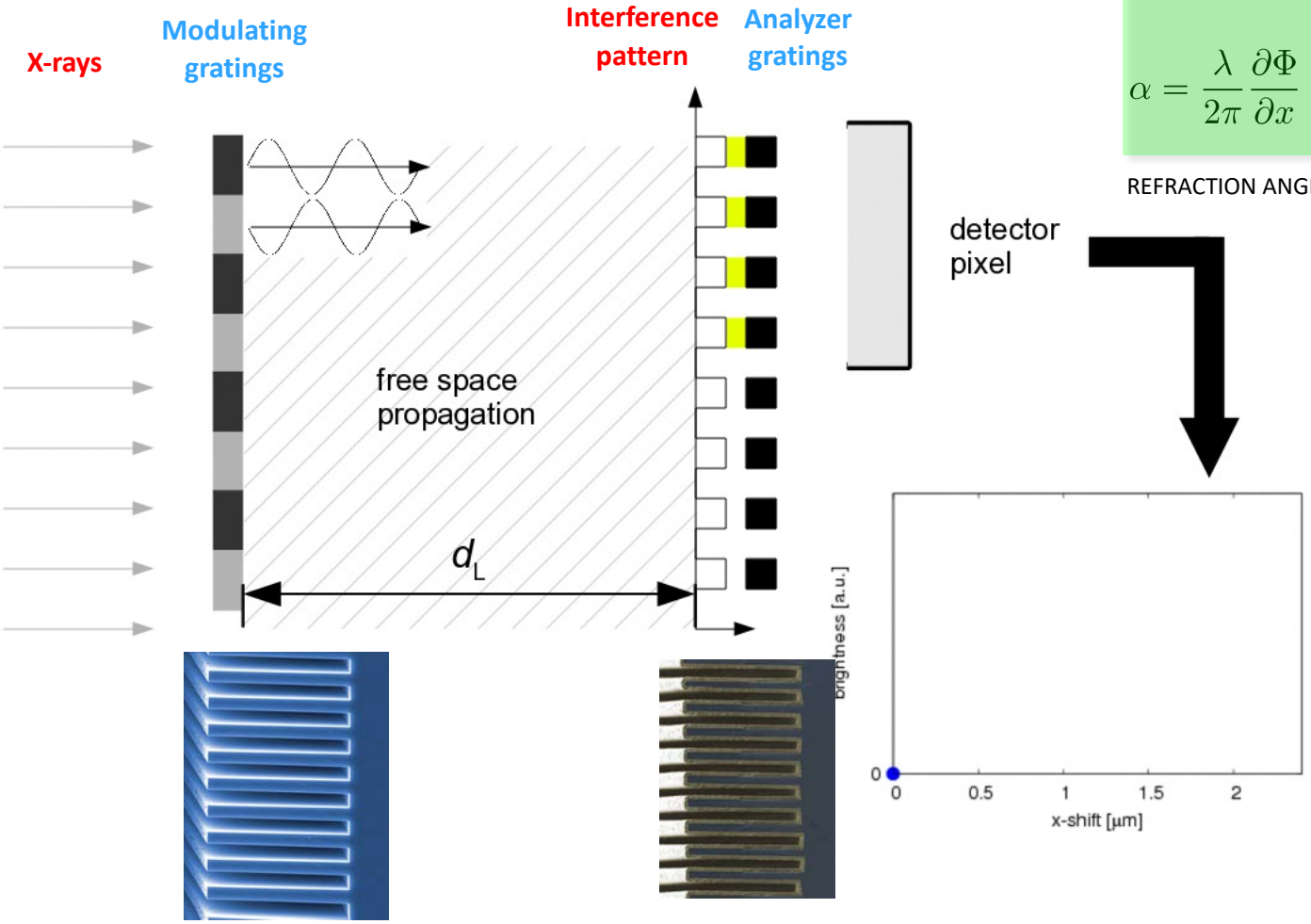

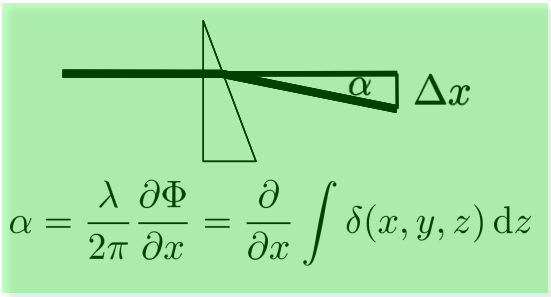

REFRACTION ANGLE of a few microradians

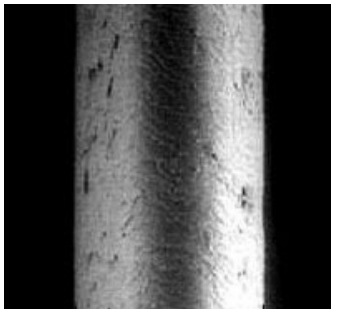

Detecting a human hair at 100m distance!

X-ray interferometry at incoherent sources

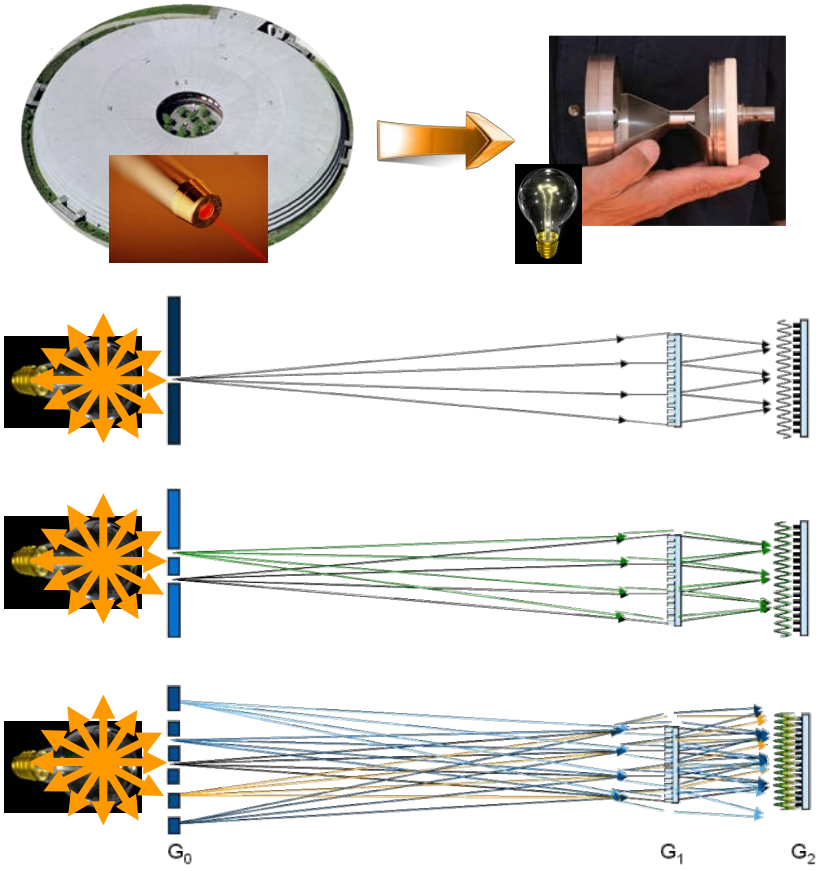

→ **Talbot-Lau interferometer**

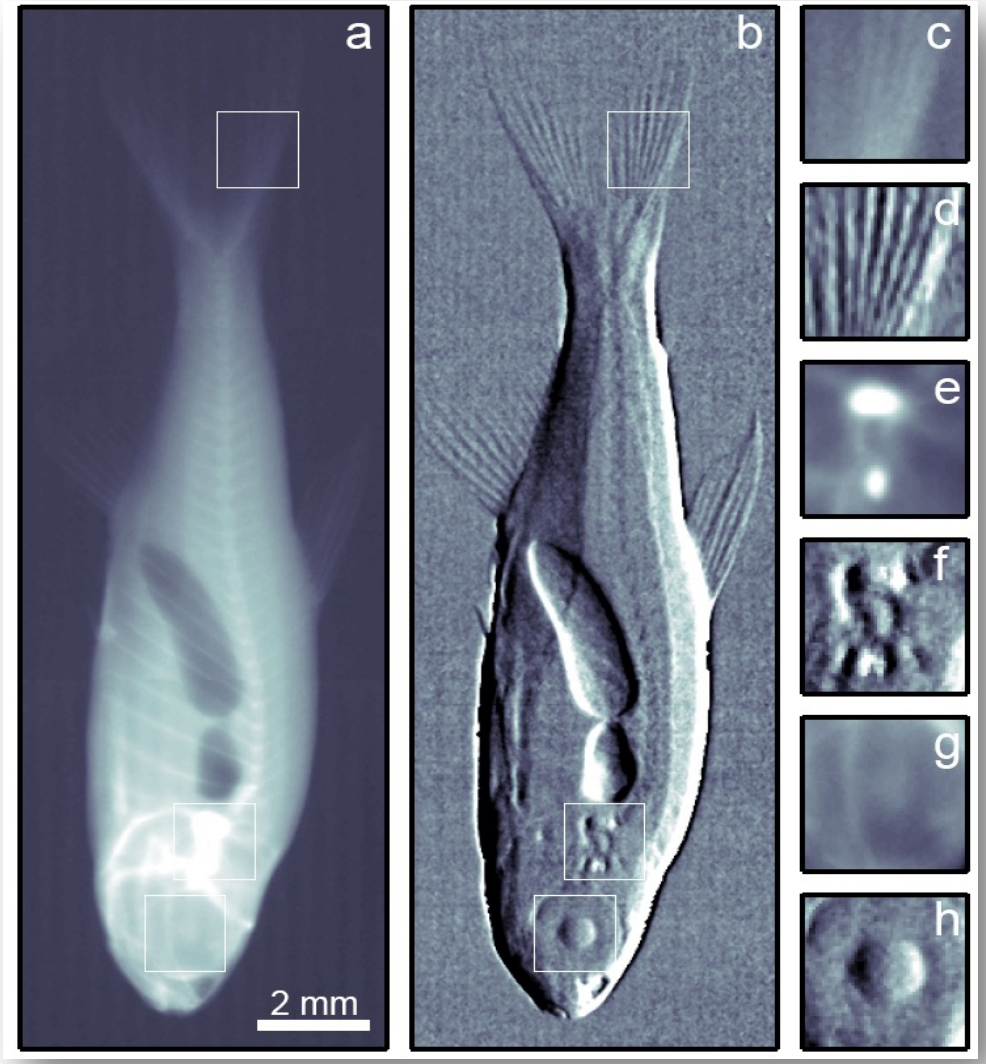

F. Pfeiffer et al., NATURE PHYSICS 2, (2006)

Vision: new radiological capabilities

Absorption image
Conventional radiography
(since 1895…)

"Differential Phase image"

"Scatter image"

Index of refraction: $n = 1 - \delta + i\beta$

Phase Absorption

PAUL SCHERRER INSTITUT PSI

Pathology 2.0: Table-top X-ray phase-contrast microtomography

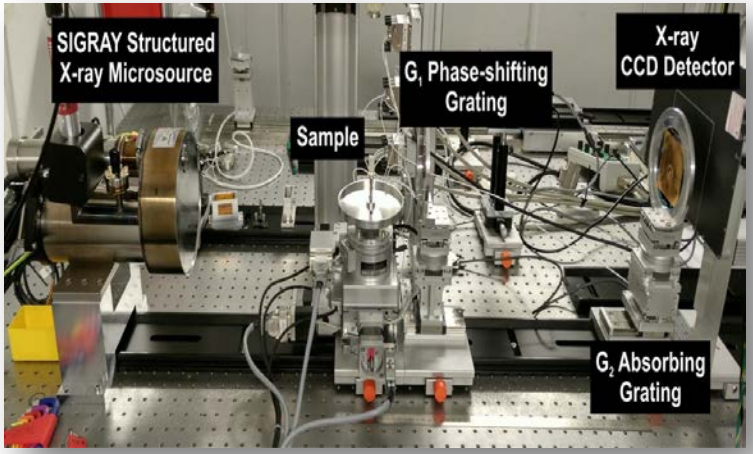

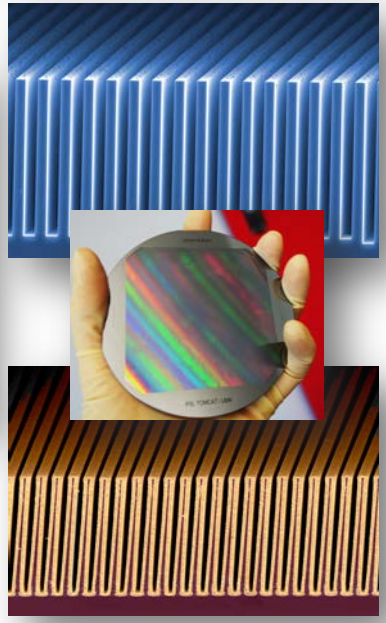

FNSNF
Fonds national suisse
Schweizerischer Nationalfonds
Fondo nazionale svizzero
Swiss National Science Foundation

J. Vila-Comamala *et al.*, "High sensitivity X-ray phase contrast imaging by laboratory grating-based interferometry at high Talbot order geometry", Optics Express (2021)

GIM : Grating interferometry mammography

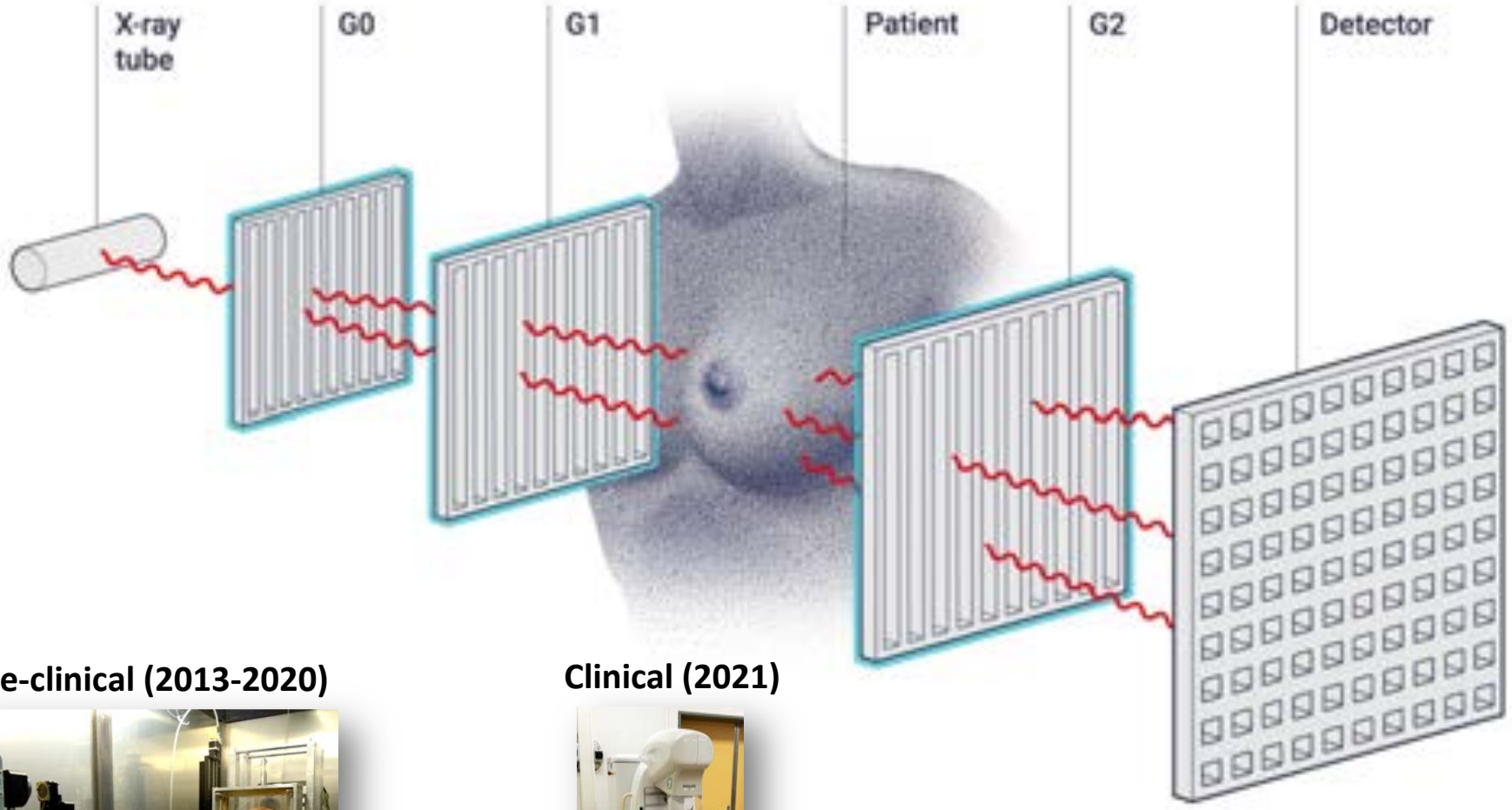

Pre-clinical (2013-2020)

Clinical (2021)

Soft tissue detection: enhanced mammography

ORIGINAL ARTICLE

A Study on Mastectomy Samples to Evaluate Breast Imaging Quality and Potential Clinical Relevance of Differential Phase Contrast Mammography

TABLE 2. Statistical Outcome Showing the Criteria Under Which mammoDPC Is Superior to Absorption-Based Mammography

Evaluated Criteria (mammoDPC Is Superior)	*P**	IQR
General quality of image	<0.001	2–3†
Sharpness and lesion delineation	<0.001	2–3
Delineation of surface structures	<0.001	2–3
Sharpness of microcalcifications	<0.001	2–2
General visibility of microcalcifications	<0.001	2–3
Potentially clinically relevant information	<0.001	4–5‡
Identification of spiculations	<0.015§	

*$P < 0.005$ is considered to be significant with Bonferroni correction.

†2 being "superior" and 3 being "equivalent" quality.

‡4 being "11% to 20% superior" and 5 being "1% to 10% superior."

§This criterion was evaluated in study 2. $P < 0.025$ is significant with the Bonferroni correction.

IQR indicates interquartile range; mammoDPC, phase cont… mammography.

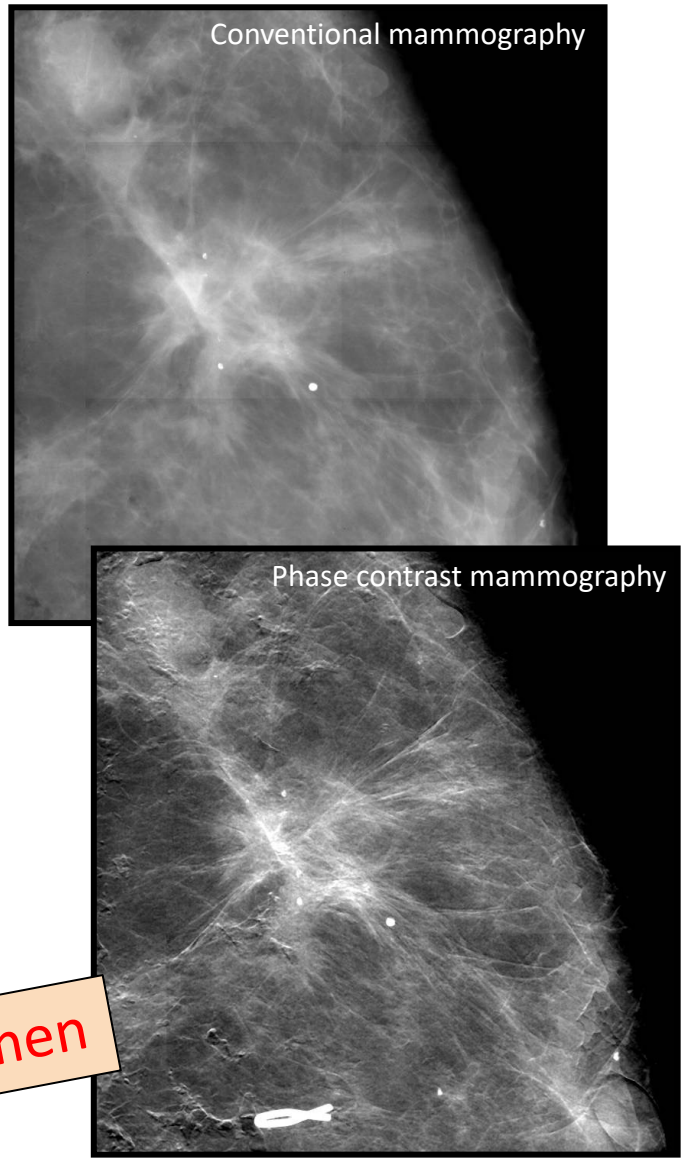

N. Hauser et al., Investigative Radiology 49 (3) 2014

Clinical translation: technical implications

FOV: 24x20 cm^2
SDD: 65-70 cm

Gratings fabrication

Scanning time of maximal 5-8s
Same (preferably less) compression force
Imaging breast thickness up to 8 cm

Acquisition protocols

Image and signal processing

Support multiple views CC/MLO
Cope with clinical routine work-out

Toolkit for design and optimizations

Dose < 1 mSv/view (EUREF)

Dose management

Pre-clinical

Clinical

Regulatory aspects

Good gratings means mastering complex nanofabrication tools

Pattern

UV Photolithography

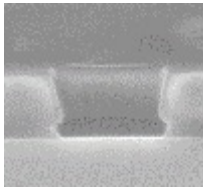

Displacement Talbot L.

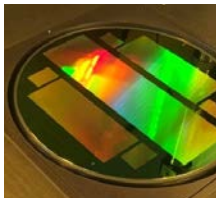

e-beam L

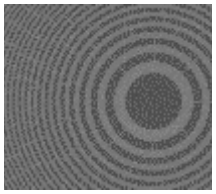

Etching

DRIE

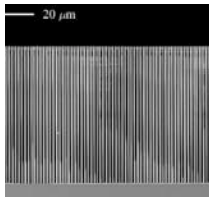

Wet-MacEtch

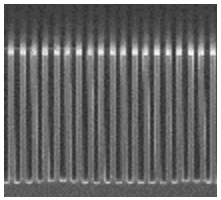

Gas-MacEtch

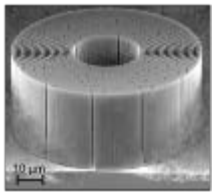

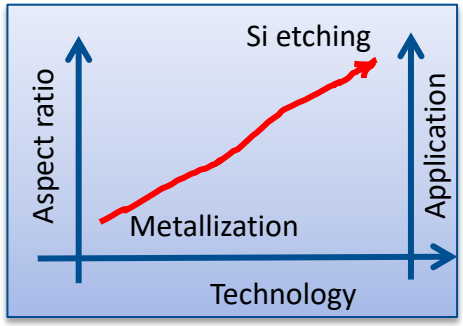

Metallization

Metal casting

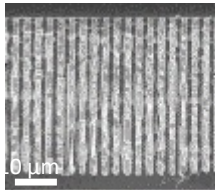

Atomic Layer Dep.

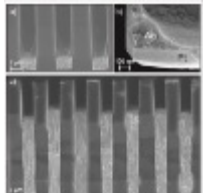

Seed growth

Au electroplating

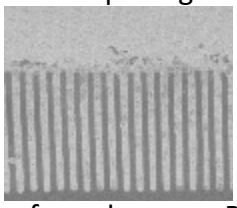

Conformal

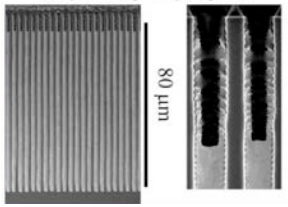

Bottom up

Testing & App.

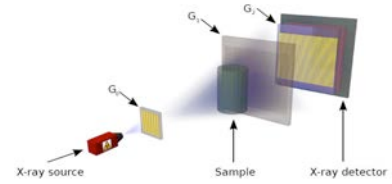

X-ray grating Interferometry

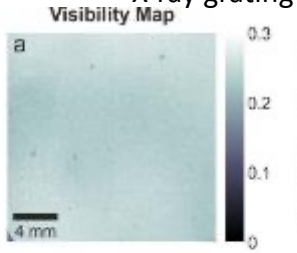

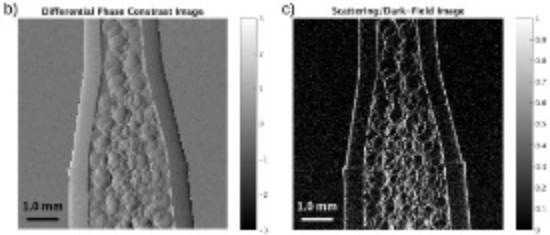

[1] Shi, Z. et al. Micromachines 11, 864 (2020).
[2] Romano, L. et al. Ad. Eng. Materials 22, 2000258 (2020).
[3] Romano, L. et al. Nanoscale Horizons 5, 869-879 (2020).
[4] Romano, L. et al. JVSTB 35, 06G302 (2017).
[5] Vila-Comamala, J. et al. Microel. Eng. 192, 19-24 (2018).
[6] Josell, D. et al. JES 167, 132504 (2020).
[7] Vila-Comamala, J. et al. Opt. Express 29, 2049-2064 (2021).
[8] Shi, Z. et al. Japanese Journal of Applied Physics 60, SCCA01 (2021).
[9] Jefimovs, K. et al. Micromachines 12, 517 (2021).

First in-man phase contrast mammography device

Arboleda *et al.*, European Radiology (2019)

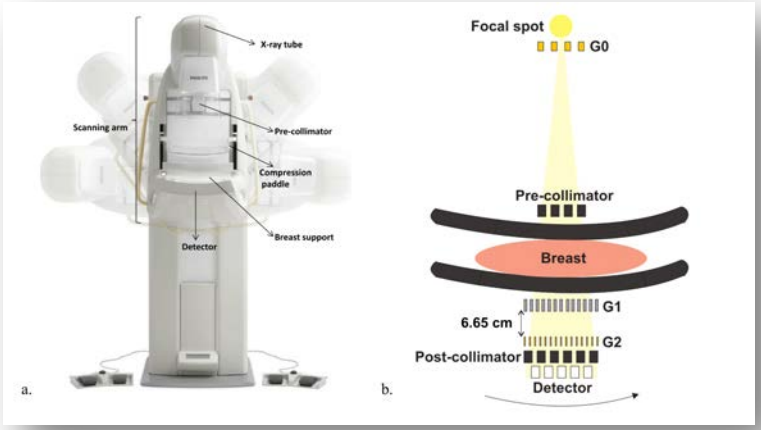

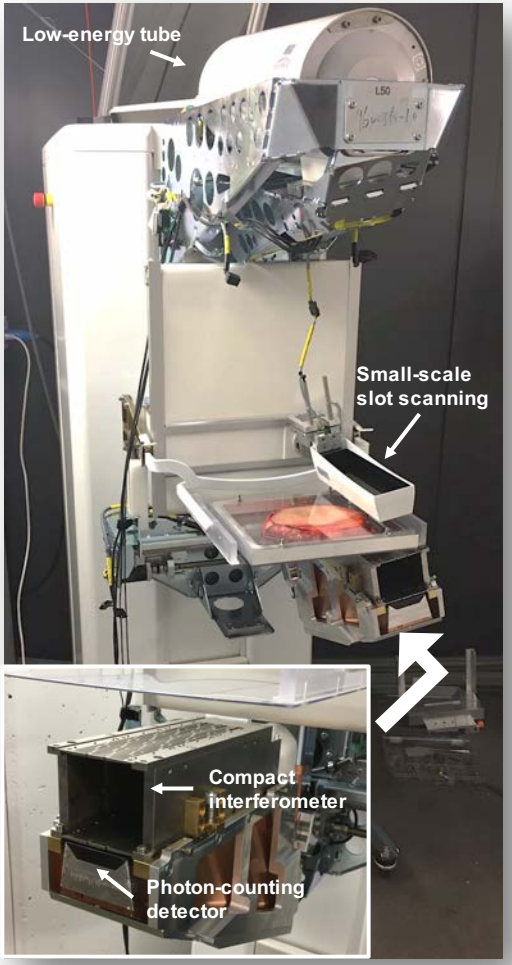

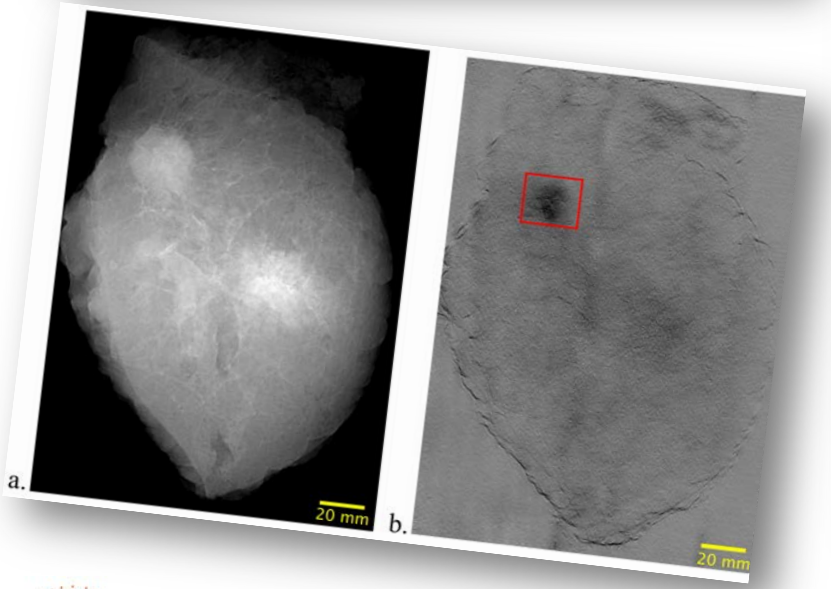

Regulatory aspects

Device recently installed at University Hospital Zürich
First pilot study ready to go!

Issues with conventional 2D breast imaging

(mammography and tomosynthesis)

N. Chotai *et al.*, Breast Imaging Essentials, (2020)

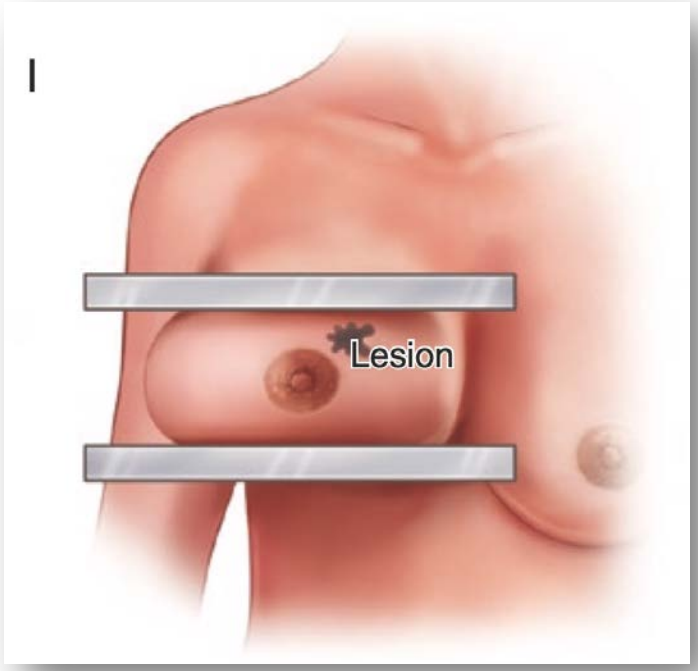

Limited contrast

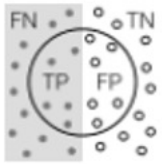

Reduced sensitivity in dense breast

Low precision ($PPV_1 < 20\%$)

Uncomfortable and painful

Need for improved breast cancer imaging technology

SWISS TECHNOLOGY AWARD INVENTORS GratXray AG 2017

Precise and painless 3D breast imaging

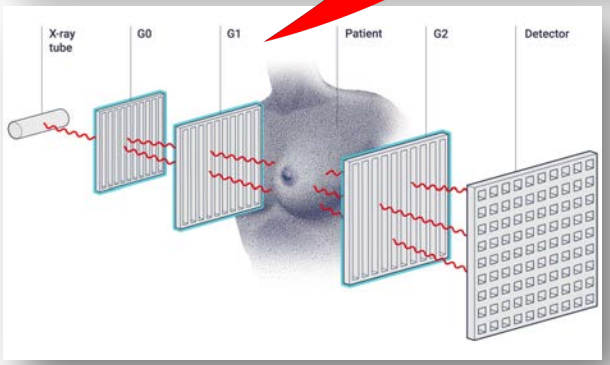

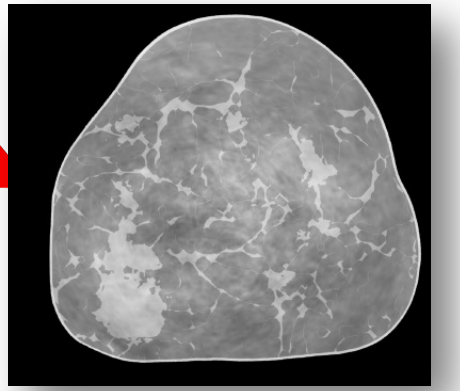

Unprecedented contrast
Excellent visibility of all tumor types

No tissue overlap (3D)
Accurate diagnosis also in dense breast tissue

No breast compression
Improved patient comfort

No contrast agent
Less side effects

From bench to bedside

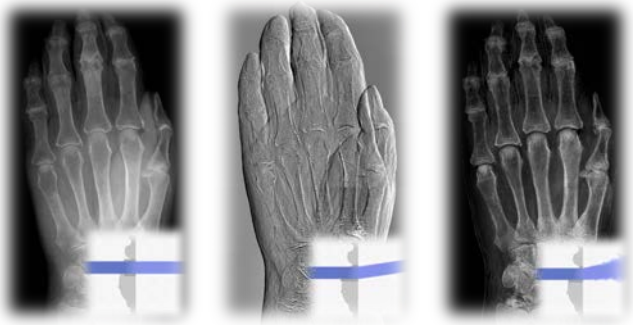

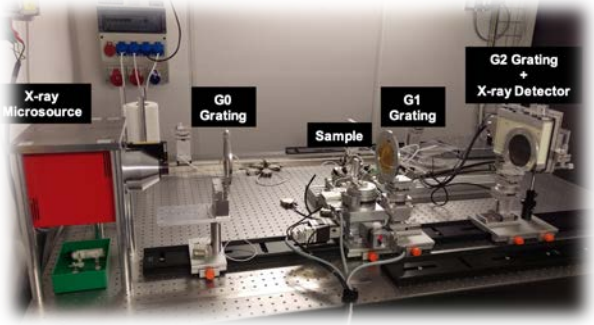

2D GI imaging
First prove of concept

3D GI imaging
First microCT application

2D GI investigational device
First patient study

2006 — 2010 — 2021

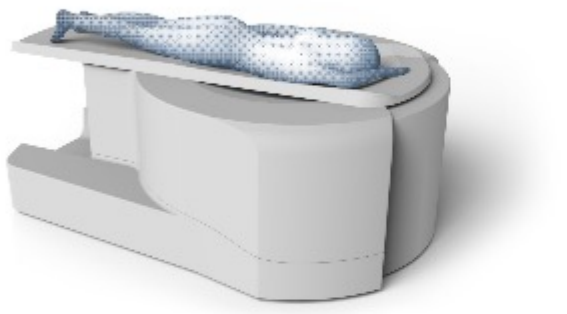

3D GI medical device

2024

SEAL OF EXCELLENCE
European Research Council
Established by the European Commission
Supporting top researchers from anywhere in the world
FNSNF
Fonds national suisse
Schweizerischer Nationalfonds
Fondo nazionale svizzero
Swiss National Science Foundation
Strategic Focus Area
Personalized Health and Related Technologies
SWISSLOS
Kanton Aargau
Fondazione Gelu
Schaan
PROMEDICA STIFTUNG

Looking into the future: TOMCAT 2.0 on SLS-2

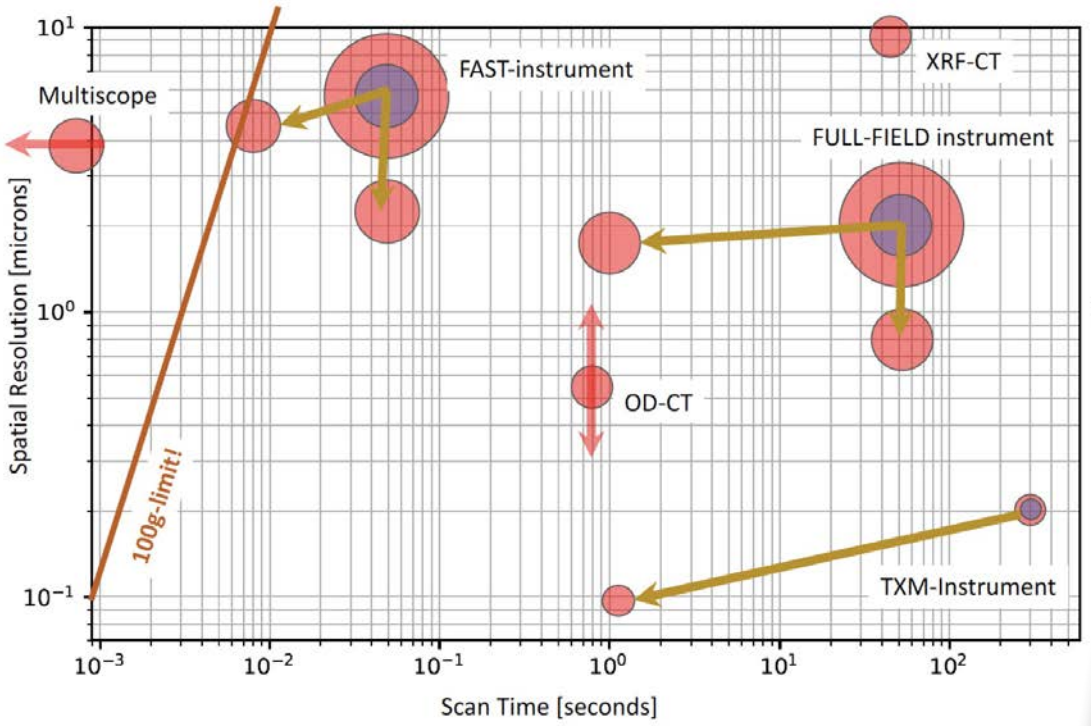

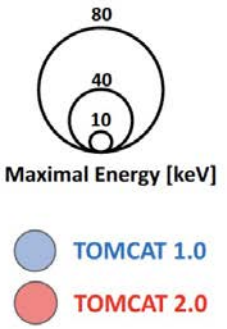

Figure 1.1: Expected development of tomographic microscopy capabilities on TC
performance of TOMCAT at the current SLS is marked in light-blue, while TOMC
SLS 2.0 are given in light-red. Brown arrows indicate expected orders-of-magnit
ment of our core instruments: a transmission X-ray microscope, a parallel-beam
a fast-imaging instrument. Expected
omnidirecti
extension o
physical lim

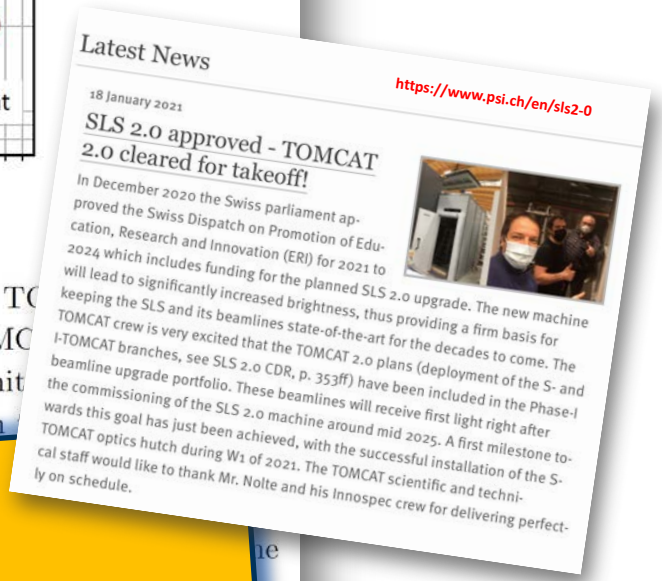

Latest News

https://www.psi.ch/en/sls2-0

18 January 2021

SLS 2.0 approved - TOMCAT 2.0 cleared for takeoff!

In December 2020 the Swiss parliament approved the Swiss Dispatch on Promotion of Education, Research and Innovation (ERI) for 2021 to 2024 which includes funding for the planned SLS 2.0 upgrade. The new machine will lead to significantly increased brightness, thus providing a firm basis for keeping the SLS and its beamlines state-of-the-art for the decades to come. The TOMCAT crew is very excited that the TOMCAT 2.0 plans (deployment of the S- and I-TOMCAT branches, see SLS 2.0 CDR, p. 353ff) have been included in the Phase-I beamline upgrade portfolio. These beamlines will receive first light right after the commissioning of the SLS 2.0 machine around mid 2025. A first milestone towards this goal has just been achieved, with the successful installation of the S-TOMCAT optics hutch during W1 of 2021. The TOMCAT scientific and technical staff would like to thank Mr. Nolte and his Innospec crew for delivering perfectly on schedule.

- Dynamic microscopy at few tens of nanometers in real-time
- Accommodate larger and denser samples
- Multimodal & multiscale tomographic imaging

→ Deploy future activities on TWO beamlines: I-TOMCAT and S-TOMCAT

TOMCAT team

Thank you!

Absorption

Phase